

## Induced Seismicity and Carbon Storage: Risk Assessment and Mitigation Strategies

28 January 2016

# Disclaimer

This report was prepared as an account of work sponsored by an agency of the United States Government. Neither the United States Government nor any agency thereof, nor any of their employees, makes any warranty, express or implied, or assumes any legal liability or responsibility for the accuracy, completeness, or usefulness of any information, apparatus, product, or process disclosed, or represents that its use would not infringe privately owned rights. Reference therein to any specific commercial product, process, or service by trade name, trademark, manufacturer, or otherwise does not necessarily constitute or imply its endorsement, recommendation, or favoring by the United States Government or any agency thereof. The views and opinions of authors expressed therein do not necessarily state or reflect those of the United States Government or any agency thereof.

This report (LLNL-TR-674138) has been reviewed by Lawrence Livermore National Laboratory and approved for public release.

**Cover Illustration:** Pressure interaction between a CO<sub>2</sub> injector and a sealing fault.

**Suggested Citation:** White, J.; Foxall, W.; Bachmann, C.; Daley, T. M.; Chiamonte, L. *Induced Seismicity and Carbon Storage: Risk Assessment and Mitigation Strategies*; NRAP-TRS-II-005-2016; NRAP Technical Report Series; U.S. Department of Energy, National Energy Technology Laboratory: Morgantown, WV, 2016; p 56.

**An electronic version of this report can be found at:**

<http://www.netl.doe.gov/research/on-site-research/publications/featured-technical-reports>

<https://edx.netl.doe.gov/nrap>

# **Induced Seismicity and Carbon Storage: Risk Assessment and Mitigation Strategies**

**Joshua A. White<sup>1</sup>, William Foxall<sup>2</sup>, Corinne Bachmann<sup>2</sup>, Thomas M. Daley<sup>2</sup>,  
Laura Chiaramonte<sup>1</sup>**

<sup>1</sup>Lawrence Livermore National Laboratory, 7000 East Avenue, Livermore, CA 94550

<sup>2</sup>Lawrence Berkeley National Laboratory, 1 Cyclotron Road, Berkeley, CA 94720

---

**NRAP-TRS-II-005-2016**

Level II Technical Report Series

28 January 2016

This page intentionally left blank.

# Table of Contents

<b>ABSTRACT</b> .....	<b>1</b>
<b>1. INTRODUCTION</b> .....	<b>2</b>
<b>2. SCIENTIFIC AND TECHNICAL BACKGROUND</b> .....	<b>5</b>
2.1    BASIC SEISMICITY CONCERNS.....	5
2.2    EVENT CHAIN VIEW OF SEISMIC IMPACTS.....	9
2.3    SITE CHARACTERISTICS.....	10
2.4    SEISMIC MONITORING.....	17
2.5    EARTHQUAKE STATISTICS.....	22
<b>3. RISK MANAGEMENT FOR INDUCED SEISMICITY</b> .....	<b>26</b>
3.1    A PHASED APPROACH TO RISK ASSESSMENT.....	26
3.2    PROBABILISTIC SEISMIC RISK ASSESSMENT.....	29
3.3    PROBABILISTIC LEAKAGE RISK ASSESSMENT.....	38
<b>4. RECOMMENDATIONS</b> .....	<b>41</b>
<b>5. REFERENCES</b> .....	<b>44</b>

## List of Figures

Figure 1: Pressure interaction between a CO <sub>2</sub> injector and a sealing fault.....	5
Figure 2: Theoretical relationship between fault rupture length (m), stress drop (MPa), and moment magnitude, assuming a circular rupture area. Shaded regions denote “typical” visibility of a fault of a given length using three-dimensional (3-D) seismic survey. Note that actual seismic resolution is highly specific to a given site and survey configuration, and should be carefully assessed. ....	7
Figure 3: Cross-section along a fault plane that intersects a CO <sub>2</sub> storage reservoir and a shallow aquifer (vertical dimension not to scale). Increased pressure in the reservoir may trigger large-scale slip on the fault, and potentially open up a leakage pathway through the caprock seals.....	8
Figure 4: Event chain view of potential impacts from induced seismicity. The open channels (or gates) represent conditions that must be satisfied for the corresponding impact (indicated by the black dots) to occur. Active and passive safeguards can be introduced along the chain to reduce the likelihood of a given condition being satisfied, and therefore reducing overall risk.....	10
Figure 5: Example faults in surface seismic data with 15 m throw (left) and 30 m throw (right). Fault is solid black line with one splay fault interpreted. Figure from the Fault Analysis Group at University College Dublin (Fault Analysis Group, 2014).....	19

## List of Tables

Table 1: Four key scenarios of concern and typical hazard and risk metrics .....	2
Table 2: Site characteristics and methods used to inform a seismic risk assessment.....	12
Table 3: Summary description of an induced seismicity risk management plan.....	28

# Acronyms, Abbreviations, and Symbols

Term	Description
1-D	One-dimensional
2-D	Two-dimensional
3-D	Three-dimensional
4-D	Four-dimensional
CO <sub>2</sub>	Carbon dioxide
DOE	U.S. Department of Energy
EGF	Empirical Green's functions
EGS	Enhanced geothermal system
EMS	European Macroseismic Scale
ETAS	Epidemic Type Aftershock Sequence
FEMA	Federal Emergency Management Agency
GCS	Geologic carbon storage
GMPE	Ground motion prediction equations
NRAP	National Risk Assessment Partnership
PISC	Post-injection site care
PLRA	Probabilistic Leakage Risk Assessment
PSHA	Probabilistic Seismic Hazard Analysis
PSRA	Probabilistic Seismic Risk Assessment
STEP	Short Term Earthquake Probability
TWT	Two-way travel time
UIC	Underground injection control
USBR	U.S. Bureau of Reclamation
VSP	Vertical seismic profiles

## Acknowledgments

This work was completed as part of the National Risk Assessment Partnership (NRAP) project. Support for this project came from the U.S. Department of Energy's (DOE) Office of Fossil Energy's Crosscutting Research program. The authors wish to acknowledge Traci Rodosta (Carbon Storage Technology Manager), Kanwal Majajan (Carbon Storage Division Director), M. Kylee Rice (Project Manager), Mark Ackiewicz (Division of CCS Research - Program Manager), Susan Maley and Steve Seachman (NETL Strategic Center for Coal), and Regis Conrad (DOE Office of Fossil Energy) for programmatic guidance, direction, and support.

## **ABSTRACT**

Geologic carbon storage (GCS) is widely recognized as an important strategy to reduce atmospheric carbon dioxide (CO<sub>2</sub>) emissions. Like all technologies, however, sequestration projects create a number of potential environmental and safety hazards that must be addressed. These include earthquakes—from microseismicity to large, damaging events—that can be triggered by altering pore-pressure conditions in the subsurface. To date, measured seismicity due to CO<sub>2</sub> injection has been limited to a few modest events, but the hazard exists and must be considered. There are important similarities between CO<sub>2</sub> injection and fluid injection from other applications that have induced significant events—e.g. geothermal systems, waste-fluid injection, hydrocarbon extraction, and others. There are also important distinctions among these technologies that should be considered in a discussion of seismic hazard.

This report focuses on strategies for assessing and mitigating risk during each phase of a CO<sub>2</sub> storage project. Four key risks related to fault reactivation and induced seismicity were considered. Induced slip on faults could potentially lead to: (1) infrastructure damage, (2) a public nuisance, (3) brine-contaminated drinking water, and (4) CO<sub>2</sub>-contaminated drinking water. These scenarios lead to different types of damage—to property, to drinking water quality, or to the public welfare. Given these four risks, this report focuses on strategies for assessing (and altering) their likelihoods of occurrence and the damage that may result.

This report begins with an overview of the basic physical mechanisms behind induced seismicity. This science basis—and its gaps—is crucial because it forms the foundation for risk assessment and mitigation. Available techniques for characterizing and monitoring seismic behavior are also described. Again, this technical basis—and its limitations—must be factored into the risk assessment and mitigation approach. A phased approach to risk management is then introduced. The basic goal of the phased approach is to constantly adapt site operations to current conditions and available characterization data.

The remainder of the report then focuses in detail on different components of the monitoring, risk assessment, and mitigation strategies. Issues in current seismic risk assessment methods that must be modified to address induced seismicity are highlighted. The report then concludes with several specific recommendations for operators and regulatory authorities to consider when selecting, permitting, and operating a storage project.

## 1. INTRODUCTION

Geologic carbon storage (GCS) is widely recognized as an important strategy to reduce atmospheric carbon dioxide (CO<sub>2</sub>) emissions (International Energy Agency, 2010; Pacala and Socolow, 2004). Like all technologies, however, sequestration projects also create a number of potential environmental and safety hazards that must be addressed. These include earthquakes that can be triggered by altering pore-pressure conditions in the subsurface. To date, measured seismicity due to CO<sub>2</sub> injection has been limited to a few modest events (Gan and Frohlich, 2013), but the hazard exists and must be addressed (National Research Council, 2012). There are important similarities between CO<sub>2</sub> injection and fluid injection for other energy technologies that have induced significant events—e.g. geothermal systems, waste-fluid injection, hydrocarbon extraction, and others. There are also important distinctions among these technologies that should be considered in a discussion of seismic risk.

This report focuses on strategies for assessing and mitigating risk during each phase of a geologic CO<sub>2</sub> storage project, and follows the general notion that *risk* consists of three parts (Kaplan and Garrick, 1981):

1. One or more scenarios of concern
2. The probability of a given scenario occurring
3. The damage that would result (i.e. consequence of the scenario)

Thus a quantitative measure of *risk* must encompass both the probability of an event and the severity of its impacts. The term *hazard* is used to refer to components 1 and 2 alone—i.e. just the probability of occurrence, without the measure of damage.

The first step in a risk assessment is identifying all plausible scenarios that may lead to damage. For a carbon storage project, four scenarios related to fault reactivation and induced seismicity should be considered. These scenarios are summarized in Table 1. Induced slip on faults could potentially lead to: (1) infrastructure damage; (2) a public nuisance; (3) brine-contaminated drinking water; and (4) CO<sub>2</sub>-contaminated drinking water. The table also provides quantitative metrics that can be used to transform the qualitative scenario descriptions into measurable hazard and risk quantities. The chosen metrics are examples, and other metrics may be preferred. Also note that hazard and risk are inherently space- and time-dependent quantities, and will evolve over the course of the project’s lifetime.

**Table 1: Four key scenarios of concern and typical hazard and risk metrics**

Scenario of Concern	Hazard Metrics	Risk Metrics
Induced earthquakes lead to	Annual probability of exceeding a given	Annual probability of exceeding a given
...structural damage	...ground motion acceleration	...structural damage level
...public nuisance	...ground motion acceleration	...nuisance level
...brine-contaminated drinking water	...volume of brine leaked to aquifer	...volume of contaminated water
...CO <sub>2</sub> -contaminated drinking water	...volume of CO <sub>2</sub> leaked to aquifer	...volume of contaminated water

The four scenarios lead to different types of damage—to property, to drinking water quality, or to the public well-being. The first scenario (infrastructure damage) is analogous to the risk associated with natural seismicity, though here the hazard results from induced events. The second scenario follows from the observation that felt earthquakes can annoy and/or scare people in the local vicinity. In this report, the common terminology “nuisance” is used for this risk, though unfortunately this word may convey the sense that it is a minor problem. The consequences should not be underestimated, however, as public backlash can lead to projects being shut down or widespread skepticism of GCS as a safe technology. The last two scenarios listed in Table 1 result from the observation that slip in a fault zone can alter its permeability structure, potentially creating or reactivating leakage pathways (Zoback and Gorelick, 2012). It is helpful, however, to make a distinction between brine and CO<sub>2</sub> leakage. While they may occur together, they have different physical behavior, likelihoods of occurrence, and groundwater impacts. In the case that other in-situ fluids are present—*e.g.*, oil or gas—additional scenarios could be added. Also, even though the process of fault reactivation, seismicity and leakage are generally closely related to each other, the occurrence of one does not necessarily imply the occurrence of the others. For example, there could be fault reactivation with aseismic slip, as well as intrinsically permeable faults that have not experienced any reactivation.

Given these four scenarios, this report focuses on strategies for assessing (and altering) their likelihoods of occurrence and the damage that may result. It should be emphasized that mitigation techniques can be applied to both aspects—*i.e.* safeguards can be put in place either to lower the likelihood of significant seismicity or to minimize damage should earthquakes occur. While it is desirable to avoid induced seismicity in the first place, the inherent complexity of subsurface systems make this a challenging task. Selection of sites having certain formation characteristics and operational procedures can be used to lower this likelihood, but an irreducible chance of triggering larger earthquakes will always remain. In light of this, it is pragmatic to always choose sites and engineering safeguards such that consequences will be low even if unwanted events occur.

The report begins with an overview of the fundamental physical mechanisms behind induced seismicity. This science basis—and its gaps—is crucial because it forms the foundation for risk assessment and mitigation. The available techniques for characterizing and monitoring subsurface behavior are also described. Again, this technical basis—and its limitations—must be factored into the assessment and mitigation approach.

Next, a phased approach to seismic monitoring, risk assessment, and mitigation is introduced. The basic goal is to constantly adapt the site operations to current conditions and available characterization and monitoring data. As the risk analysis evolves, so too do monitoring and potential mitigation plans. In early stages of a project—particularly pre-injection—data limitations can make overly detailed assessments ill-constrained and inaccurate. The site analyses must therefore be updated and improved as new information comes in. Also, all carbon storage projects are heavily cost-limited, and monitoring budgets must be allocated judiciously. A baseline seismic monitoring and assessment plan is likely sufficient for many projects, to confirm that the seismic risk is low and that operations are proceeding as expected. If a particular site begins to exhibit symptoms of concern, however, a more rigorous monitoring and assessment plan must be quickly put in place. These contingencies must be thought about in advance, as a quick response is a key component of mitigation.

The remainder of the report focuses in detail on different components of the monitoring, assessment, and mitigation strategies. Current seismic risk assessment methods are highlighted that must be modified to address induced seismicity. This report then concludes with several specific recommendations for operators and regulatory authorities to consider when selecting, permitting, and operating a storage project.

This report focuses primarily on the case of injection of supercritical CO<sub>2</sub> into a deep, saline aquifer. Saline storage has a large resource potential, and will likely form a significant portion of the carbon storage inventory. Most of the discussion also applies to other storage types—e.g. CO<sub>2</sub> enhanced oil recovery—though some specifics with respect to lithology, in situ fluids, and reservoir pressure conditions may change.

## 2. SCIENTIFIC AND TECHNICAL BACKGROUND

This section provides an overview of scientific and technical issues that impact the proposed risk management approach. It begins with a high-level discussion of the basic mechanisms controlling induced seismicity. The discussion then explores in detail the site characteristics, monitoring techniques, and operator decisions that have an impact on seismic risk.

### 2.1 BASIC SEISMICITY CONCERNS

Figure 1 provides a conceptual example of the basic seismicity concern. Here, a vertical well injects supercritical CO<sub>2</sub> into a storage reservoir. The reservoir is intersected by a moderately large, pre-existing fault. As injection begins, a CO<sub>2</sub>-rich plume grows away from the injector, driven by pressure gradients and buoyancy forces. As the injected fluid displaces the in situ brine, a large overpressure plume also develops. Note that the extent of the pressure perturbation is typically much larger than the CO<sub>2</sub>-rich plume. This pressure perturbation plume can interact with the fault, and potentially trigger seismic or aseismic slip. In this example, the fault is drawn as a hydrologic barrier, though non-sealing faults present the same concern.

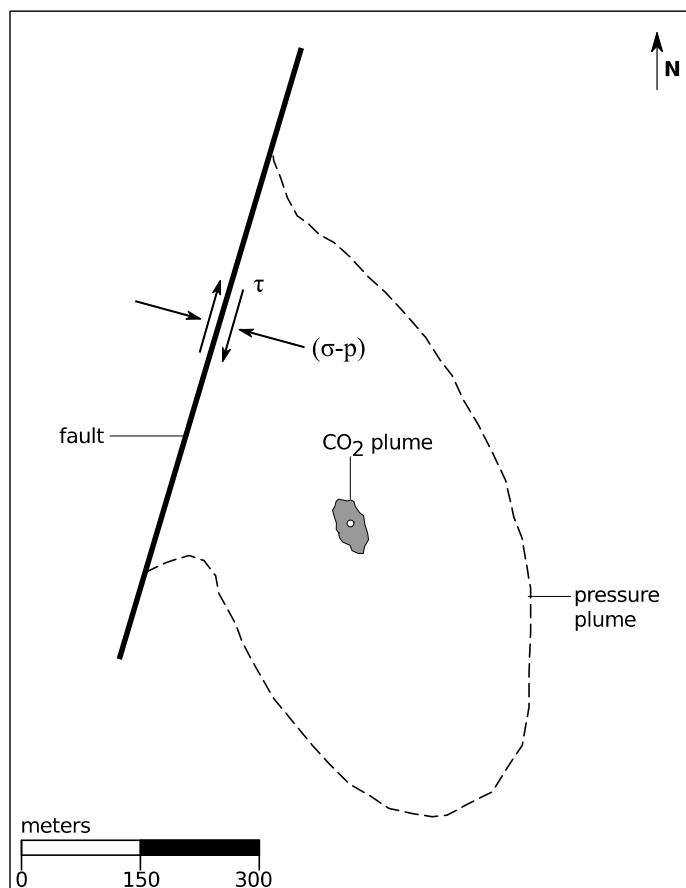


Figure 1: Pressure interaction between a CO<sub>2</sub> injector and a sealing fault.

A simple Coulomb criterion can be used to express the condition for fault stability,

$$\tau \leq \mu(\sigma - p). \quad (1)$$

Here,  $\tau$  and  $\sigma$  are the *total* shear and normal tractions applied on the fault,  $p$  is the pore fluid pressure, and  $\mu$  is the static friction coefficient. The geomechanical convention is that positive stresses are compressive. The quantity  $(\sigma - p)$  represents the *effective* normal traction on the fault, which is reduced by an increase in pore pressure. Due to the isotropic nature of pore pressure stress, the pore pressure has no impact on the shear component. The stability condition states that the fault will be stable as long as the shear traction is less than the shear strength mobilized by the effective normal confinement.

The shear and normal tractions resolved on a fault plane will depend on the in situ state of stress in the formation, and on the orientation of the fault with respect to this stress state. For a given state of stress, some faults may be favorably oriented for slip, while others may be poorly oriented. A simple measure of fault stability is therefore the critical pore pressure change  $\Delta p$  required to make condition (Equation 1) an equality. It is commonly observed that many faults are naturally in a state of critical equilibrium, in which the equality condition is nearly satisfied under in situ stresses and formation fluid pressures (Zoback and Zoback, 1980). Very small perturbations in stress or pore pressure therefore can trigger slip. It is these critically-stressed faults that pose the greatest challenge for subsurface fluid injection (Zoback and Gorelick, 2012).

Equation 1 is a useful model in practice, though it hides much of the underlying complexity of the system. For example, it ignores poromechanical and thermomechanical effects, which may substantially alter the state of stress (Segall, 1989). It ignores additional strength that may result from cohesion and fault geometry effects. Also, note that this criterion is expressed as a point-wise condition, whereas in reality the stability of the fault will depend on a distribution of stresses, pressures, and friction strength across the whole surface. Finally, this condition only describes the behavior of the fault while it is in static equilibrium. Once slip is initiated, a whole host of mechanisms come into play to dissipate built-up strain energy. The fault may creep (quasi-static slip) aseismically until it reaches a new stable configuration or until it ruptures dynamically in an earthquake. The slip behavior is largely controlled by the evolution of the friction coefficient as a function of the slip velocity and state of the fault (Dieterich, 1979; Dieterich and Kilgore, 1994; Ruina, 1983) (see Section 3.2.2). Fault ruptures may also exhibit complex foreshock, mainshock, and aftershock behavior. Furthermore, while adaptation of Equation 1 to include time-dependent evolution of the friction coefficient is useful for understanding the earthquake nucleation process, it does not describe important aspects of dynamic rupture once an earthquake is underway.

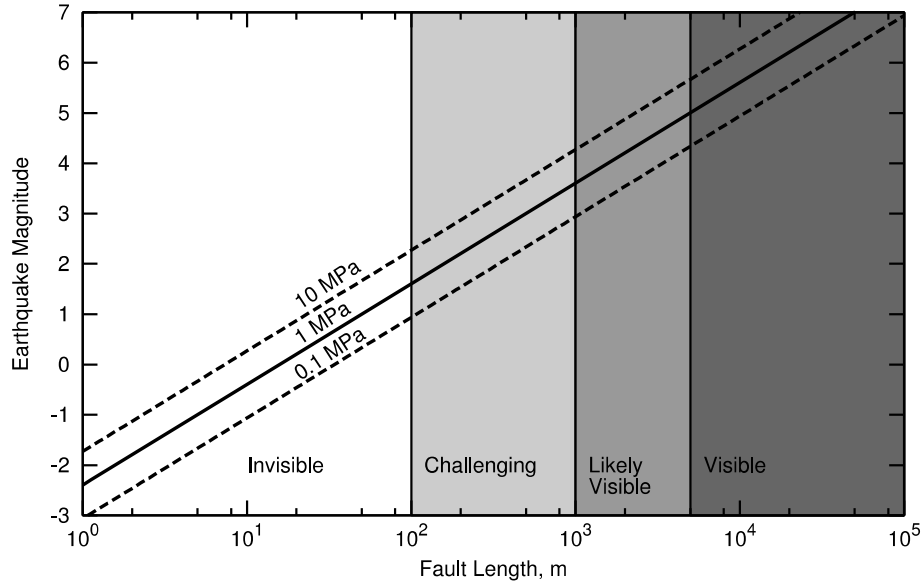


**Figure 2: Theoretical relationship between fault rupture length (m), stress drop (MPa), and moment magnitude, assuming a circular rupture area. Shaded regions denote “typical” visibility of a fault of a given length using three-dimensional (3-D) seismic survey. Note that actual seismic resolution is highly specific to a given site and survey configuration, and should be carefully assessed.**

The primary factor controlling the maximum magnitude event that a fault can produce is its area. In Figure 1, for example, the fault is large enough to generate significant earthquakes. Figure 2 illustrates a theoretical relationship between rupture diameter, stress drop, and moment magnitude (Hanks, 1977; Scholz, 2002). This relationship assumes an idealized circular rupture geometry—reasonable for modest earthquakes—so that fault length (diameter of the idealized fault area) may be related to the maximum possible rupture area. In this example, the fault length (1 km) and a commonly observed range of stress drops (0.1 to 10 MPa) indicate a potential  $M_{\max}$  of  $3.6 \pm 0.7$ . Such events could be felt by nearby populations and possibly cause damage to seismically-fragile infrastructure in the immediate vicinity. The fault is also sufficiently large that the rupture area could fully or partially breach a caprock seal over several hundred meters (Figure 3). The major concern is that shear-slip on faults and fractures can alter permeability and possibly open up new leakage pathways within the fault zone. Of course, the actual seismic and leakage hazard will depend on a number of site-specific factors, many of which are discussed in the next few sections.

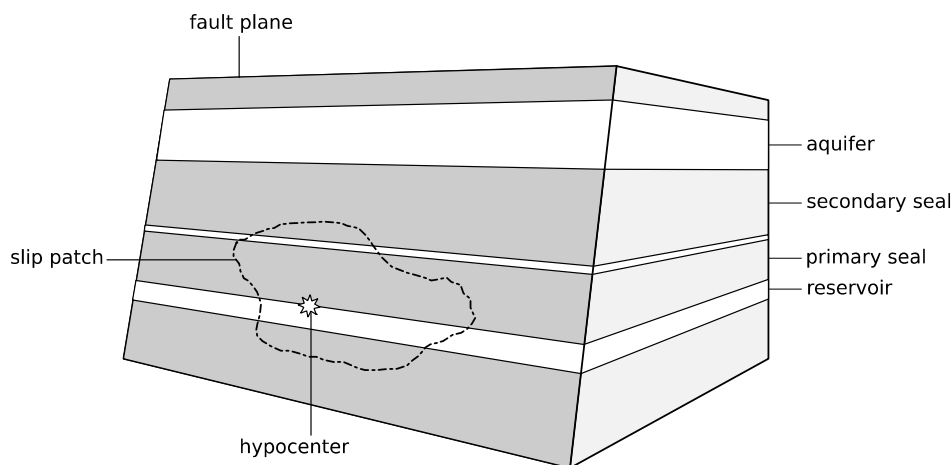


**Figure 3: Cross-section along a fault plane that intersects a CO<sub>2</sub> storage reservoir and a shallow aquifer (vertical dimension not to scale). Increased pressure in the reservoir may trigger large-scale slip on the fault, and potentially open up a leakage pathway through the caprock seals.**

While the fault in this example is large enough to produce seismicity of concern, it is also sufficiently small that it could potentially be missed in a three-dimensional (3-D) seismic survey. Figure 2 also shows an indication of “typical” fault visibility, though actual seismic resolution is highly site- and survey-specific. Fault visibility is primarily determined by whether the fault creates substantial vertical offsets on reflecting horizons. Small, low-offset, and/or steeply dipping faults are particularly difficult to see with reflection seismic. Basement faults and stratigraphic units having widely-spaced reflectors are also challenging. Strike-slip faults may have substantial accumulated displacement but little vertical offset. While one can site the injector away from observed faults that are considered well-oriented for slip, there is an unavoidable chance that the pressure plume will encounter smaller, unobserved faults that can still create seismicity of concern.

The issue of 3-D seismic resolution is crucial for a carbon storage project to consider, as it divides pre-existing faults into two important populations: observed and unobserved. Observed faults are by definition larger and could potentially generate damaging events. At the same time, their visibility means that operators can plan for them during the site selection and project design phases. High-risk faults would simply be avoided, and low-risk faults would be carefully monitored. Unobserved faults are smaller and therefore less capable of generating events of concern. Since the primary concern is the risk of nuisance from smaller events that occur relatively frequently, rather than structural damage, the invisibility of smaller faults prior to injection poses a real challenge from a risk mitigation point of view. Certain site characteristics can be used as a guide to identify storage sites with lower seismicity potential, but some irreducible risk of re-activating smaller faults will always persist. The only way to obtain information about such faults is to carefully monitor microseismicity and the pressure behavior of the field as injection proceeds.

Given the inherent importance of identifying faults that may interact with the pressure plume, a careful (and conservative) assessment of seismic resolution and the structural geology at a given site is necessary to place an upper bound on the size of unknown faults.

## 2.2 EVENT CHAIN VIEW OF SEISMIC IMPACTS

A storage project is a complex system, and a number of conditions must align in order for a particular impact to occur—*e.g.*, a building being damaged, or a drinking water resources being contaminated. Figure 4 provides a simple event-chain view of induced seismicity, describing a few key conditions that must be satisfied for one of the four risk scenarios described earlier to occur. This perspective is useful because many of these conditions provide an opportunity for engineering safeguards to be put in place. By reducing the likelihood that any of these conditions will be satisfied—either through site selection, monitoring, or operational procedures—the overall risk can be reduced.

It is also helpful to recognize that some of these conditions are easier to address than others. As mentioned earlier, it is impossible to guarantee in advance that the pressure plume will never encounter faults capable of generating significant seismicity. Careful site selection and characterization can be used to reduce the hazard, but it can never be eliminated. An obvious goal should therefore be to choose storage sites that can tolerate fairly large earthquakes without leading to significant consequences.

For example, consider a carbon storage site that is located far from population centers, or in a region with stringent building code standards. In this case, the risk of infrastructure damage is low, even if a worst-case event should occur. Similarly, storage sites are typically chosen because they have resilient, widely-spaced caprock sealing layers. By selecting sites with limited potential leakage pathways and relying on multiple seals, the likelihood of brine or CO<sub>2</sub> contamination of a shallow aquifer can be kept low even if larger events were to occur. Most carbon storage projects to date have adopted this multi-layered approach to risk management, in which overall risk is reduced by combining multiple safeguards that reinforce one another.

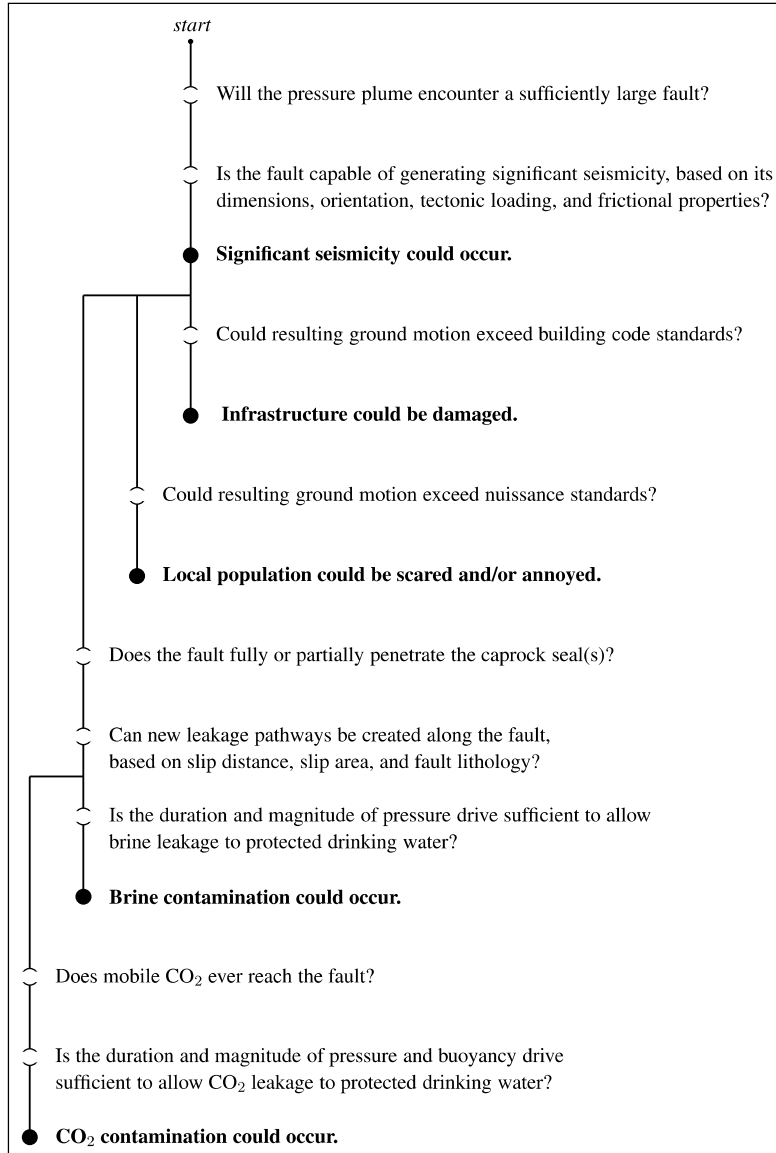


**Figure 4: Event chain view of potential impacts from induced seismicity. The open channels (or gates) represent conditions that must be satisfied for the corresponding impact (indicated by the black dots) to occur. Active and passive safeguards can be introduced along the chain to reduce the likelihood of a given condition being satisfied, and therefore reducing overall risk.**

### 2.3 SITE CHARACTERISTICS

Carbon storage operations require the collection of a wide variety of geological data to assess the site storage capacity and to assure that storage performance and safety criteria can be met. The goal is to describe the geology, hydrogeology, geochemistry, and geomechanics of the selected site (Benson et al., 2005). Traditionally, the main emphasis has been placed on describing the reservoir and overlying seals. Given recent concerns about the potential for induced seismicity (Zoback and Gorelick, 2012), a thorough characterization is also needed to assess the potential

for fault and/or fracture-reactivation and resulting consequences. This requires a comprehensive analysis of the complete system, including the underburden, reservoir, overburden, and surface conditions.

Table 2 summarizes site-specific characteristics and data sets that can inform both seismic and leakage risk assessments. The properties most useful for understanding the fluid flow, geomechanical, and seismic behavior of a storage site are included. The table also provides a brief list of methods commonly used to measure these properties. Some are straightforward to measure— *e.g.*, vertical stress—while others are notoriously difficult to estimate—like fault permeability. Like all subsurface projects, challenges associated with uncertainty, heterogeneity, and measurement length-scales must also be addressed. A major goal of the ongoing carbon storage pilot projects in the U.S. and elsewhere is to identify cost-effective techniques for estimating these properties and using them to forecast field behavior.

**Table 2: Site characteristics and methods used to inform a seismic risk assessment**

Category	Characteristics	Primary Methods
Structure	Stratigraphy	Reflection seismic, drilling logs
	Faults	Reflection seismic, microseismic, well tests, geologic mapping, mud losses
Stress	Fractures	Borehole imaging, mud losses, structural inferences, well tests, core
	Vertical stress	Density log
	Min horizontal stress	Leak-off test, extended leak-off test, mini-frac
	Max horizontal stress	Borehole breakout, tensile failure observations
	Pressure	Drillstem test, wireline tools, gauges, reflection seismic
	Temperature	Wireline tools, gauges
Poromechanics	Elastic properties (static and dynamic)	Core, sonic logs
	Compressive and tensile strength	Core
	Thermal expansion	Core
	Fracture cohesion, friction, dilation	Core
	Fault frictional properties	Core, outcrops, lithologic inferences
	Matrix permeability, porosity	Core, log and seismic inferences, history-matching
Fluid Flow	Fracture permeability, aperture, connectivity	Core, history-matching
	Fault permeability	Lithologic inferences, interference testing
	Injection rate, pressure, temperature	Wellhead and bottom-hole sensors
	Background seismicity	Microseismic array, regional arrays
	Injection-related seismicity	Microseismic array
	Tectonic regime	Local and regional assessment
Seismicity	Velocity and attenuation model	Velocity analysis, calibration shots, VSP, seismic tomography
	Hydrologic properties	Piezometers, core, history-matching
	Geochemistry	Core, lithologic inferences
	Water-quality	Water-sampling
	Soil conditions	Site geotechnical assessment, VS30 assessment
	Infrastructure fragility curves	Structural assessment
Surface Impacts	Community sensitivity	Questionnaires, townhalls, and other public forums

The next few sections examine the most relevant site characteristics in detail.

### **2.3.1 Site Characteristics that Impact Fault Reactivation**

The likelihood of fault reactivation and significant seismicity will depend on a number of factors. The central goal of the characterization effort is to evaluate the most important controls on the seismic potential of the site. These include:

1. *In situ stresses.* Fault slip is controlled by the normal and tangential tractions applied along the fault plane. A top priority must therefore be to estimate the *in situ* stress state at the site and its variation with location and depth. Building on existing stress compilations, well tests, well logs, and geomechanical modeling can be used to estimate the three *in situ* principal stresses—usually the vertical stress, minimum horizontal stress, and maximum horizontal stress—and determine if a fault in a given orientation is likely to be reactivated (using Equation 1 or more sophisticated extensions). The *in situ* stress field can also be estimated from earthquake focal mechanisms, although generally with higher uncertainty than from well measurements. Typically the magnitude of the vertical stress and the direction and magnitude of the minimum horizontal stress can be determined with high confidence, while estimating the maximum horizontal stress is harder and less certain. Practical methods for determining the *in situ* stress state are discussed in detail in Zoback et al. (2003). Note that the *in situ* stress controls much of the geomechanical behavior of the field, beyond just fault reactivation, and it is therefore a valuable investment to devote time and budget to pinning these values down.
2. *Location, size, and orientation of faults.* In order to understand fault slip potential, it is necessary to calculate the normal and shear components of the stress resolved on each portion of the fault. Maximizing the accuracy of fault locations and orientations is therefore critical for such assessment. Reflection seismic surveys are one of the better tools to identify pre-existing faults. However, reflection data are not usually effective in delineating faults with small offsets or that intersect few horizons. The other significant tool is microseismic observations. Ongoing microseismicity can sometimes be used to identify otherwise undetected faults that pose a risk of generating larger earthquakes. Finally, faults often serve as either hydrologic barriers or flow conduits. Pre-existing faults may therefore have a noticeable impact on the fluid pressure measured at the wellbore(s). Pressure falloff testing and similar well tests can be used to identify barriers and flow conduits, particularly if they are located in the near-wellbore region—e.g. (Bourdet, 2002).

Other sources of information may also be available in certain instances. Larger faults may have surface expressions that can be mapped. Wellbore imaging can provide information on faults and fractures that intercept the wellbore, and is particularly useful when the fault is penetrated by multiple wells. Structural geology studies can provide information on the deformation style, expected faulting regime, and expected patterns.

While it is often difficult to constrain individual faults, fault populations tend to follow well-established statistical distributions in terms of their size and density. It is sometimes possible to constrain these distributions, at least partially, using available data. In particular, if a data set is available on the frequency of larger faults—i.e. from 3-D seismic or regional surveys—it may be possible to extrapolate the observed distribution to estimate the likely density of medium-sized, sub-seismic-resolution faults. The inferred

density can then be used within probabilistic hazard assessments. Jordan et al. (2011) present an interesting analysis along these lines, using fault density statistics to examine the probability that pressure and/or CO<sub>2</sub> might encounter faults during a previously planned injection in the San Joaquin Basin. The same approach could be easily extended to consider the seismicity hazard.

3. *Fault structure and previous loading history.* Detailed information about faults is difficult to obtain in practice, and their behavior upon reactivation is challenging to predict. Large uncertainties will therefore invariably enter into the hazard analysis, as is generally the case for Probabilistic Seismic Hazard Analysis (PSHA). Wellbore image logs or core through the fault zone are the best way to obtain direct observations, but can only be obtained if the well passes through a fault. Well observations are also inherently limited to a one-dimensional (1-D) view along the wellbore trajectory. Some information can be inferred from structural geology studies that take into consideration the rock types that the fault intersects and its deformation style. Information on the previous loading history of faults through regional tectonic history can also aid fault stability analysis. In very active tectonic regions the long-term slip rates and characteristic coseismic slip magnitudes of outcropping seismogenic faults can be estimated from paleoseismic investigations.
4. *Mechanical properties of the host rocks, fractures, and faults.* CO<sub>2</sub> storage reservoirs will mostly be situated between 800–3,000 m depth (Eiken et al., 2011). Shallow sedimentary units are more ductile than deeper basement rocks, and also tend to be more heterogeneous. Indeed, observations of natural tectonic seismicity shows that earthquake frequency tends to increase with depth in the shallow crust (Sibson, 1982). It has also been observed that Gutenberg-Richter *b*-values tend to decrease with depth in many regions; that is, at greater depths one tends to observe a higher proportion of large magnitude events compared to smaller ones (Gerstenberger et al., 2001; Mori and Abercrombie, 1997). Mori and Abercrombie (1997) hypothesized that larger heterogeneity at shallow depths—in both material properties and stress distribution—make it more likely for ruptures to be arrested before growing into large events. Marone and Scholz (1988) also proposed that the transition to predominantly aseismic slip and the tendency towards small events results from the slip-strengthening frictional properties of fault gouge at shallow depths (at least in mature faults) compared with the slip-weakening behavior at greater depths needed for nucleation of larger earthquakes. Nevertheless, moderate magnitude events are observed at depths shallower than 5 km and remain a concern.

Lab tests on cores and core plugs can give direct information on the mechanical properties of rocks, though the issue of scaling from lab measurements to field behavior is always problematical (Barton, 1976). These tests can measure the bulk behavior of intact rock or the behavior of fractures in the samples. Lab measurements also often serve as reference data to calibrate empirical correlations of well log data.

Recent work by Kohli and Zoback (2013) used triaxial experiments on fractured shale to assess the effect of clay content on friction coefficient, frictional stability, and dilation properties. Their results suggest that slip in shales with less than ~30% clay will propagate unstably (i.e. slip-weakening) and generate seismic events, whereas slip in

shales with more than ~30% clay will occur stably (i.e. slip-strengthening), generating low frequency, long duration sub-seismic slow slip events, as observed by Das and Zoback (2013). Because shale units are commonly used as confining layers, this work has important implications for the seismic and leakage behavior at storage sites. It also highlights the fact that a lack of microseismic observations does not necessarily imply that no reactivation is occurring.

5. *Pore pressure perturbation.* Induced events are triggered by pressure perturbations that relieve the normal confinement on faults, and therefore a good understanding of the evolving pressure distribution in the reservoir and surrounding formation is essential. The primary method to determine the pressure distribution is to perform history-matching with a reservoir simulator, using available field data as a constraint. Reservoir modeling is a mature practice, and will obviously be a major focus during the planning and operation stages of the project. The pressure evolution will depend on reservoir geometry, fluid and rock properties, flow barriers, compartmentalization, and so on. The goal is to identify faults that may experience overpressure during the lifetime of the field, and the subset that may come in contact with mobile CO<sub>2</sub>. Note that the permeability of the fault (both across-fault and along-fault) will play a role in determining the zone of pressurization. If a fault is intrinsically impermeable, the zone of pressurization will likely be confined to the reservoir interval alone. If the fault is intrinsically permeable in-plane or has been previously reactivated, pressure may migrate upwards or downwards along the fault plane. It may even reach intersecting faults at deeper or shallower depths. It should be kept in mind, however, that the zone of pressurization—*i.e.*, the fault patch within which an induced event may be *nucleated*—is distinct from the entire area of the rupture patch that may slip during a seismic event. The dynamic rupture is largely controlled by the release of pre-existing strain energy stored in the surrounding rock volume, and may extend beyond the pressurized zone. The details of this rupture process, and its relationship to the pressure plume, are complex and an area of active research.

Locations of induced microearthquakes may be useful in tracking the growth of the pressure front, particularly if events are observed in unexpected locations—say, below or above the storage interval. This latter technique assumes, however, that location uncertainties are sufficiently small. Indeed, a good understanding of the intrinsic location uncertainty is essential to making informed decisions based on microseismic observations.

6. *Thermal and poroelastic effects.* While fault stability is often assessed assuming a simple Coulomb criterion, Equation 1, this simple relationship ignores stress perturbations that may result from thermal and poroelastic effects. Relevant properties—elastic moduli, Biot coefficient, thermal expansion coefficient, thermal diffusivity—can be estimated using laboratory experiments or logging tools. It is generally observed that cooling—from injecting cold CO<sub>2</sub>—attenuates quickly with distance from the well, and so poroelastic effects are dominant in the far-field. Slightly more sophisticated calculations can be used to include these effects. In practice, however, coupled hydromechanical simulations are most useful.

### **2.3.2 Site Characteristics that Impact Ground Motion and Damage**

The likelihood of generating significant ground motions—and damaging/annoying events—will depend on:

1. Source magnitude and mechanism
2. Distance to sensitive populations and/or infrastructure
3. Seismic velocity and attenuation properties of the subsurface
4. Shallow soil and bedrock properties
5. Building design standards
6. Local level of “comfort” with non-damaging but felt seismic events

Methods for assessing the seismic fragility for a given site are well-established from historical experience with natural seismic hazards (see Section 3.2.4). Some subtle distinctions, however, exist between natural and induced hazards that should be considered in the seismic risk assessment process. These issues are discussed in detail in Section 3.2.

### **2.3.3 Site Characteristics that Impact Leakage Pathways**

The likelihood of contaminating a protected aquifer with brine or CO<sub>2</sub> will depend on:

1. Degree to which the fault penetrates hydrologic seals
2. Area of induced slip (rupture patch)
3. Whether, and to what degree, fault zone permeability increases after slip
4. Barrier effectiveness and mitigating effects of secondary seals or thief zones
5. Duration of pressure drive in the reservoir
6. Whether mobile CO<sub>2</sub> comes in contact with the new leakage pathway
7. Effectiveness of any active mitigation or remediation measures deployed

Item 6 is important when considering the relative risk of brine vs. CO<sub>2</sub> contamination. As the maximum areal extent of the mobile CO<sub>2</sub> plume is typically much smaller than the pressure perturbation plume, the likelihood of generating a brine-only leakage pathway is proportionally higher. That said, the buoyant nature of supercritical CO<sub>2</sub> in brine can make it more difficult to mitigate a CO<sub>2</sub> leak than a brine leak. Also, in certain reservoir configurations CO<sub>2</sub> may ultimately migrate to areas that never experience a substantial pore pressure increase.

Most of the factors mentioned above can be understood with traditional characterization data sets that are required during the initial stages of a sequestration project. A critical but challenging part of the leakage risk assessment, however, is evaluating whether new leakage pathways can be created by fault slip. The hydromechanical behavior will be controlled by the structure and lithology of the fault itself and surrounding damage zone. For that purpose, direct observation of structure and properties are desirable, but are rarely obtained in practice. In the absence of direct measurements, fault zone permeability values (pre-slip) have traditionally been estimated in the oil and gas industry using a variety of approaches that incorporate deformation mechanism, host rock lithology, presence of clays, diagenesis, stress, etc. (Wibberley et al., 2008). These estimates can help establish a baseline scenario, and some indication of the leakage potential.

Natural seeps or underfilled gas traps in the area may also provide evidence of fault leakage under in situ conditions.

A few field studies have analyzed the interaction between pore pressure, strain, and seismicity. For example, Guglielmi et al. (2008) performed a small injection into a 30-m-wide shallow fault, while concurrently acquiring pressure, strain, seismic, and in situ permeability measurements. Even though this type of dedicated study is impracticable for most storage sites, small-scale field experiments are useful to understand prototypical behavior of fault zones.

Given difficulties in estimating fault permeability, the conservative assumption that a fault can form a leakage pathway may be warranted unless contravening evidence exists. This uncertainty underscores the need to choose sites that minimize potential leakage pathways to sensitive aquifers through faults. If a large, known fault penetrates the sealing layers and is considered a plausible hazard, above-zone pressure monitoring could be deployed to watch for pressure perturbations in a permeable layer between the storage reservoir and protected drinking water. Active mitigation mechanisms, such as hydraulic barriers, may also be deployed if an actual leak is detected, though the cost and effectiveness of these measures will be highly site-specific.

## **2.4 SEISMIC MONITORING**

Monitoring of site-specific seismicity is essential to understanding risk and how it varies with time. There are two major types of seismic monitoring: passive monitoring of earthquakes and other sources, and active source monitoring employed in seismic reflection and refraction surveys. Passive earthquake monitoring includes both measurement of strong ground shaking and weak motion from small and/or distant earthquakes. Triggered accelerometers are typically deployed to measure strong ground motion, whereas local and regional seismometer networks are used to measure ground velocity waveforms over a wide dynamic range from both microearthquakes and larger events. This section focuses on (1) active source seismic reflection surveying and (2) local microseismic monitoring.

Monitoring seismicity at GCS sites has much in common with monitoring of other subsurface operations, including geothermal energy production and hydraulic fracturing for oil and gas production. There is a wealth of technical/scientific literature and commercial expertise available to support seismic monitoring. This section focuses on unique aspects of monitoring design at a GCS field.

Ideally, GCS monitoring begins as part of site characterization. Both passive and active seismic monitoring should be considered in initial designs. If a regional seismic network encompasses the storage area, data from it can provide a natural seismicity baseline. In most cases, the regional data will have a minimum detection threshold of (roughly) M2.5 to 3.0, which is useful for identifying major faults, but does not have the resolution of site-specific monitoring. Ideally, a 3-D surface seismic survey will also be obtained early during site characterization. This is typically done to define geologic structure and aid lithological characterization. 3-D seismic can locate faults via their disruption of subsurface structures, and thus serve as a guide for design of further monitoring.

### **2.4.1 3-D and 4-D seismic**

The use of active-source seismology for resource exploration and engineering studies began in the early 20th century and has progressed to basin-scale 3-D imaging of seismic reflectivity and subsequent analysis for subsurface properties. Since the 1990's, 3-D surface seismic has progressed into time-lapse monitoring—i.e. four-dimensional (4-D) seismic—providing a tool for imaging changes in subsurface conditions.

Surface seismic data can be two-dimensional (2-D, sources and sensors recorded on a line) or 3-D (recorded on a grid). Additionally, sensors can be placed in wells (borehole seismic) to produce vertical seismic profiles (VSP), which can be 2-D (sources on a line) or 3-D (sources on a grid). The primary use of both surface seismic and VSP is to image the reflections from interfaces in the subsurface. The reflection images are then interpreted for subsurface structure, lithology and physical properties (such as fluid content). VSP is also used to directly measure the seismic velocity structure of a site, which is an important constraint on all seismic imaging and monitoring. For purposes of monitoring induced seismicity, the first use of reflection imaging is detection of faults that could activate and cause seismic events. The visibility of faults (the extent to which they can be resolved or interpreted on a given seismic data set) is, to first order, controlled by the offset induced in reflecting interfaces.

An example of fault interpretation from offset interfaces is shown in Figure 5. These images are reproduced from the Fault Analysis Group at University College Dublin (Fault Analysis Group, 2014). They show an interpreted splay fault with 15 or 30 m of throw (offset). The figure shows a “time-section” in which the vertical axis is two-way travel time (TWT) and the horizontal axis is distance. An important property of surface seismic is that it measures travel time, not depth directly, so there is always some uncertainty in the vertical scale. The time-to-depth conversion is performed using a model of subsurface seismic velocity for the site, which is always subject to a degree of uncertainty. This uncertainty can be reduced by using well data, e.g. VSP, to measure directly the velocities of rock layers along the well. GCS projects will typically not have many wells available, so the uncertainty in depth may be a factor in determining fault offsets. As fault throw becomes smaller, identification becomes more difficult. Also, if the offset is pure shear, parallel to layering (no vertical component), the fault may not be observed on surface seismic. Similarly, faults within basement rock are difficult to detect because there may be few or no offset reflectors.

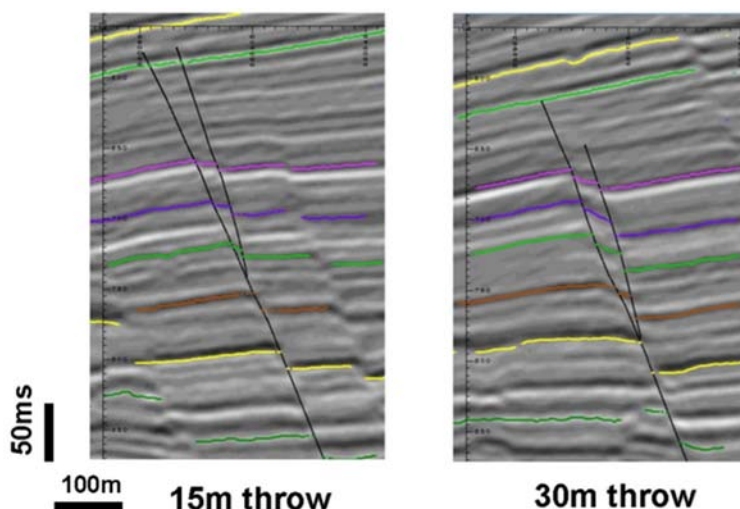


**Figure 5: Example faults in surface seismic data with 15 m throw (left) and 30 m throw (right). Fault is solid black line with one splay fault interpreted. Figure from the Fault Analysis Group at University College Dublin (Fault Analysis Group, 2014).**

To observe vertical offsets in reflections, a common estimate of resolution is one-fourth of a wavelength, where the seismic wavelength is a function of data frequency content and wave velocity. The data in Figure 5 is relatively high frequency, with the 15 m offset being about one wavelength and easily observed. More typical surveys have wavelengths of 50–100 m, giving a quarter wavelength of 12–25 m.

There are more advanced techniques to identify faults and fracture zones in reflection seismic data than simple offset of bedding planes. Several seismic “attributes” are used to identify more subtle characteristics, especially in 3-D data volumes. Most of these attributes are based on identifying some disruption to the seismic wave propagation and mapping that disruption. In most cases, these attributes are calibrated or constrained by direct subsurface measurement from boreholes. Forward modeling can also be used to increase confidence in interpretation.

Seismic monitoring can also potentially be used to detect changes in pressure and CO<sub>2</sub> saturation. Detectability is highly site specific, however, and dependent on rock properties and data quality. Again, the best results are obtained when well control data are available. If there is no direct subsurface constraint, such as a monitoring well, then estimates of pressure and fluid saturation can be affected by variation of other subsurface properties. Well data are needed to understand rock properties such as porosity and matrix compressibility that affect the seismic response to fluids. Also, as the distance from well control increases, subsurface heterogeneity causes increasing uncertainty in property estimates.

A key factor in the use of active-source seismic monitoring, both surface and borehole, is cost. Cost is highly variable, and it is difficult to give generalized estimates. The costs depend on location (onshore or marine), land access, permitting and regulatory control, size of area to be imaged, data quality and spatial sampling required, depth range to be imaged, surface conditions, weather conditions, etc. There are many commercial providers offering surface and borehole seismic services. It is, however, important to have seismic and geophysical expertise within the

GCS project team. Design, acquisition, processing, and interpretation all benefit from knowledgeable oversight, which in turn can help control costs.

### **2.4.2 Microseismic Monitoring**

Present-day earthquake monitoring networks cover most of the Earth's continental area at station spacings varying from a few to hundreds of kilometers, and large data sets are publically available. However, permanent networks are fairly sparse and are often supplemented with temporary deployments. Processing and analysis of network data has generally reached a level of sophistication that often includes automatic detection and first-pass event location and other analyses, and near-real time transmission of the results via the internet and telephone paging.

The main components of microseismic monitoring are array design, deployment/operation, and data analysis. Note that microseismic monitoring installations are typically arranged in "networks" or "arrays," composed of multiple recording stations. A local network will usually have centralized data collection and, ideally, be homogenous in instrumentation for consistency. Unless it can be established conclusively in advance that a GCS site has sufficiently low risk of induced seismicity, it will be prudent to establish a baseline microseismic monitoring network. The network should first be used to characterize background seismicity before any subsurface activity begins. While the time needed to establish a background level is site dependent, a period of at least 6 months should be considered as a minimum.

An important point of comparison for GCS microseismic monitoring is related experience with enhanced geothermal systems (EGS). The U.S. Department of Energy (DOE) EGS Program has developed an internationally reviewed and accepted management protocol and recommended best practices for monitoring and assessing induced seismicity (Majer et al., 2012a,b). The conclusions and recommendations include:

1. The seismic monitoring program should strive to collect data that are not biased in time or space in the vicinity of the potential project
2. Minimum data processing should provide the location, magnitude and source mechanisms
3. The monitoring should be maintained throughout the injection activity to validate the engineering design of the injection in terms of fluid movement directions, and to guide the operators on optimal injection volumes and rates

Within the EGS protocol it is understood that seismic events represent both an operational and nuisance hazard, with the nuisance hazard being important to public outreach efforts. One advantage of microseismic monitoring is that it can be automated and reported to the public as a matter of course, just as natural earthquakes are monitored, analyzed and reported in near-real time.

### **Array Design**

The above goals are relevant to a GCS project, and a key factor in achieving success is the array design. The design process should begin by defining the spatial extent of the subsurface to be monitored and the resolution required for event location (both in space and magnitude). For example, if the expected pressure plume has a 1-km radius, the project should have a monitoring array with a 2–3 km radius so that the expected seismicity is located within the array perimeter.

Locating events typically requires a minimum of four seismic recording stations. A single recording station can record ground motion, but it cannot be used to determine location or magnitude with any precision, nor can it easily discriminate natural events from background noise (*e.g.* construction, traffic, etc.). The spacing of the stations in a network is usually on the same scale as the area to be monitored. Uncertainty in event location and size increases significantly as one moves outside the perimeter of the monitoring stations. Better networks will have at least 10–12 stations for moderate to high-level precision in location and magnitude. If concerning seismicity is encountered, projects should consider deploying additional stations to improve coverage and precision. Temporary surface stations can also be deployed relatively quickly as an intermediate measure.

Individual stations use seismic sensors (seismometers, geophones, accelerometers) and either local recording and/or data transmission to a central recording site. The sensors should be three-components, allowing measurement of the full vector wavefield. The instruments used should have bandwidth appropriate to their location. Deep borehole sensors, such as in a monitoring well, may observe frequencies up to 1 kHz or more, while shallow (30–100 m) borehole stations can observe hundreds of Hz, and surface deployments are typically limited to a maximum of 100–200 Hz. The magnitude threshold detectable for deep, shallow or surface deployment is similarly controlled. While surface stations typically have a minimum detection threshold of M0 to M1, the thresholds in shallow and deep boreholes are often M0 to M-1 and M-2 to M-3, respectively. Increasing the signal-to-noise ratio by placing sensors below the immediate ground surface (below the weathering layer and water table) is often the most cost effective improvement that can be made in network design. Observing the relatively large numbers of smaller magnitude events (those not representing an actual hazard) that occur is used to develop an understanding the geomechanical processes controlling potentially larger seismicity. The sensitivity of a proposed network configuration can be assessed via modeling studies, although uncertainty in the subsurface structure places limits on the precision of the results.

### **Processing and Interpretation**

The precision in depth location is controlled primarily by the lateral spacing of the recording stations and accuracy of the subsurface seismic velocity model. Like active source seismic data, microseismic data are recorded as a waveform time series and subsurface velocities are needed to convert arrival times to event locations. Unlike active-source data, the origin time, location and mechanism of the earthquake source are unknown and determining those source attributes is the primary objective. With data of sufficient quality and quantity, both source attributes and a velocity model can be determined from the data. The source properties reported will, at a minimum, include the magnitude (energy), time, and location of the source. If there is a significant seismicity concern, then the data analysis should include moment tensor analysis, which provides deeper understanding of source mechanisms. An important goal of the location analysis is to determine if coherent structures such as fault planes can be resolved. For example, if events appear to be located along a plane, then the possibility of a previously unknown fault should be considered. The automation of data analysis can also allow near-real time integration of injection data and thus allow mitigation measures to be developed to mitigate the occurrence of larger events (see Section 3.2).

## 2.5 EARTHQUAKE STATISTICS

Earthquake statistics are used to describe and model the occurrence of seismic events. Empirical laws describe the relationship between event size and frequency of occurrence. Although these laws are determined based on natural seismicity, recent studies of geothermal induced seismicity (Deichmann and Giardini, 2009) and seismicity in mines (Kwiatek et al., 2010) indicate that they hold for these cases as well.

### 2.5.1 The Gutenberg-Richter Law

The cumulative number of earthquakes  $N$  in a given volume above magnitude  $M$  generally follows a power law distribution and can be expressed as (Gutenberg and Richter, 1942),

$$\log N = a - bM \quad (2)$$

where  $a$  and  $b$  are constants. The  $a$ -value describes the productivity, or the long-term mean rate of occurrence of all earthquakes above some reference magnitude. The  $b$ -value describes the relative size distribution. Higher  $b$ -values indicate more small events relative to larger events. The fitting of the  $a$ - and  $b$ -values depends on the magnitude down to which the seismic catalog is considered complete (the magnitude of completeness  $M_c$ ). One of the major factors influencing this magnitude is the network design, as described earlier.

The above distribution is usually truncated at the estimated maximum magnitude for the region. Earthquake occurrence on individual fault segments often follow the Gutenberg-Richter law at lower magnitudes, but may exhibit distinctly enhanced frequencies around larger “characteristic” earthquakes (Ben-Zion, 2008; Schwartz and Coppersmith, 1984) that rupture across essentially the entire segment. Characteristic earthquakes appear to occur more frequently than predicted by extrapolating the linear Gutenberg-Richter plot from lower magnitudes. In this case, the frequency-magnitude relation is modified to account for the enhanced occurrence rates around the characteristic earthquake (Youngs and Coppersmith, 1985).

The Gutenberg-Richter relationship is used in most hazard analyses to estimate the occurrence frequencies of earthquakes of different magnitudes (the frequency-magnitude distribution). The spatial and temporal variations of  $b$ -values have been the topic of several studies, ranging from worldwide variations (e.g. Gulia and Wiemer, 2010; Schorlemmer et al., 2005) down to laboratory studies (Amitrano, 2003, 2012). High  $b$ -values have been linked to the presence of fluids in studies in subduction zones (van Stiphout et al., 2009) and volcanic systems (Wiemer and Wyss, 1997). In recent studies (Bachmann et al., 2012; Bachmann et al., 2011; Goertz-Allmann and Wiemer, 2012),  $b$ -values of induced seismicity of a geothermal project were studied in detail. The authors found that the highest values are generally seen at the beginning of an injection as many small events are triggered. The  $b$ -values decline with time and with distance from the injection point. These studies indicate that there is a relationship between the  $b$ -value and the magnitude of the local pore pressure perturbation. The authors argue that large changes in pore pressures lead to high  $b$ -value as many small events are triggered that would not be triggered from tectonic loading alone. Conversely, smaller pore pressure changes lead to lower  $b$ -values as they trigger mostly events that were already closer to failure.

### 2.5.2 The Omori-Utsu Law

The Omori Law was first introduced to describe the decay of aftershock series in Japan. It was later modified to the Omori-Utsu law (Ogata, 1999; Utsu, 1961) which is generally used today. This law describes a Poisson process with time that indicates how long it will take for the seismic activity to decay to background activity after a large seismic event:

$$\lambda(t, M_c) = \frac{k(M_c)}{(t + c)^p}$$

where  $\lambda$  is aftershock frequency,  $t$  is the time elapsed after the main shock,  $c$  and  $p$  are empirical parameters, characteristic for a specific sequence, and  $k(M_c)$  is a function of the number of events with magnitudes above the completeness magnitude  $M_c$ . Studies based on geothermal induced seismicity in Basel, Switzerland and Soultz, France (Bachmann, 2011; Bachmann et al., 2011) also indicate that this law can be used to describe the decay of the seismicity after fluid injection has been terminated. When the background seismicity at the project site is known, it can be used to estimate how long the disturbance caused by the fluid injection will last. This can give a general time frame for the long-term monitoring of a site. This law also forms the basis for several statistical models of induced seismicity.

### 2.5.3 Statistical Models

There are a variety of statistical models that can be applied to the occurrence of induced seismicity. Most of these models have originally been developed to forecast ongoing natural seismicity, especially aftershock series. These models use empirical parameters fitted to the seismic sequence to forecast the behavior of the sequence in the very near future, often the next 6 to 24 hours. To adapt these models to induced seismicity, injection parameters can be incorporated into the model. Three potentially useful models have previously been used to forecast induced seismicity. The application of these statistical forecast models is discussed in Section 3.2.2.1. It should be noted that these models are essentially empirical in nature, and their connection to the underlying physics of pressure propagation and fault reactivation can be weak. Nevertheless, they have proven successful in modeling the observed behavior of many field studies. Current work by many groups is focused on improving the physical basis of these short-term forecasting models.

Two commonly used models to forecast and describe aftershock sequences are the Short Term Earthquake Probability (STEP) and the Epidemic Type Aftershock Sequence (ETAS) models. The basis of both models are the Gutenberg-Richter behavior and the Omori-Utsu type decay. The STEP model is based on a simple aftershock model of (Reasenber and Jones, 1989)

$$\lambda(t, M_c) = \frac{10^{A+b(M_m-M_c)}}{(t + c)^p}$$

where  $A$  is given as

$$A = A_0 - \log\left[\int_s^T (t + c)^{-p} dt\right]$$

$$A_0 = a - bM_m$$

Here,  $a$ ,  $b$ ,  $p$  and  $c$  are the same constants as in the Gutenberg Richter law and the Omori-Utsu law.

While the STEP model treats every earthquake as an individual that increases the probability of the following earthquakes, the ETAS model incorporates cascades of multiple generations of earthquake interactions. There are different approaches to the application of the ETAS model. The first application to induced seismicity by (Bachmann et al., 2011) used the model of (Ogata, 1988). The rate of aftershocks induced by an event occurring at time  $t$  with magnitude  $M_i$  is given by

$$\lambda_{i(t)} = \frac{K}{(t + t - t_i)^p} 10^{\alpha(M_i - M_{min})}$$

for time  $t > t_i$ . The parameters  $c$  and  $p$  are empirical parameters, and  $K$  and  $\alpha$  describe the productivity of the sequence. The total occurrence rate is the sum of the rate of all preceding earthquakes and a constant background rate  $\lambda_0$ :

$$\lambda(t) = \lambda_0 + \sum_{i:t < t_i} \lambda_i(t)$$

The authors include the injection flow rate  $F_r$ , by adding a term to the background rate. According to Shapiro and Dinske (2009), the fluid-triggered event rate can be modeled as being proportional to the injection rate:

$$\lambda_0(t) = \mu + c_f F_r$$

with  $c_f$  and  $\mu$  being free parameters.

Shapiro et al. (2010) introduced a new model that is solely used for induced seismicity. They introduce the seismogenic index  $\Sigma$ , which depends on the tectonic potential of the injected region. The tectonic potential was introduced by (Shapiro et al., 2007); it is a measure of the tectonic activity of a site. The authors defined it as the upper limit of the critical pressure of pre-existing cracks divided by their bulk concentration. A larger tectonic potential indicates that more effort is needed to induce microseismicity. The value can depend on, e.g., the stress state, tectonic history, rheology, lithology, heat flow, and natural seismicity at the project site. They combine it with the Gutenberg-Richter law to determine the number of events:

$$\log N_m(t) = \log Q_c(t) - bM + \Sigma$$

where  $M$  is the magnitude,  $b$  is the  $b$ -value of the Gutenberg-Richter law and  $\Sigma$  is the seismogenic index and  $Q_c$  is the injected fluid volume.

### **3. RISK MANAGEMENT FOR INDUCED SEISMICITY**

This section focuses on the essential ingredients of a risk management strategy for induced seismicity during GCS. A phased-approach to the risk management plan is introduced, one that adapts to current site conditions and available characterization data. With this general strategy in hand, the ingredients of a full Probabilistic Seismic Risk Assessment (PSRA) are described that can be used to address the infrastructure damage and public nuisance risk scenarios described earlier. In parallel, a Probabilistic Leakage Risk Assessment (PLRA) can be used to address the brine and CO<sub>2</sub> leakage risks.

#### **3.1 A PHASED APPROACH TO RISK ASSESSMENT**

A carbon storage project can be broken into several stages of operation:

1. *Site-screening*. This is the initial site assessment phase, when a number of alternative locations and injection horizons are considered. Typically the available characterization data are quite limited, unless a site is already being used for other purposes—e.g. oil and gas development, or previous injection operations.
2. *Pre-injection*. During this stage, baseline characterization is performed at the selected site. An underground injection control (UIC) permit is obtained, and one or more wells are drilled. Up to this point, available monitoring data are limited, covering a relatively short baseline period.
3. *Injection*. This is the primary operation period, during which CO<sub>2</sub> is injected and a suite of field monitoring data are collected at regular intervals
4. *Stabilization*. This period covers the end of injection until the reservoir stabilizes—that is, pressure perturbations have returned to near baseline levels, and all mobile-phase CO<sub>2</sub> is structurally trapped. Some level of post-injection site care (PISC) will persist until site liability is transferred or released.
5. *Mitigation and remediation*. While this stage is hopefully unnecessary for the vast majority of GCS projects, active mitigation and/or remediation may be necessary if a significant seismicity problem is encountered. This stage therefore encompasses any significant deviation from planned operations to address unexpected problems.

Induced events can occur at any time while overpressure persists. Once the pressure returns to baseline levels, the induced hazard mostly disappears. The one caveat is that the complexities of stress transfer on faults can lead to aftershocks. These processes are initiated during the pressurized period, but new ruptures can persist for some time after the pressure decline. Also, the background tectonic hazard will always persist.

The time window of concern for the first three risk scenarios listed in Table 1 (infrastructure damage, public nuisance, brine leakage) covers the entire overpressure period and some additional period to allow for aftershock decay. The same is mostly true for the fourth scenario (CO<sub>2</sub> leakage), as an induced event is required to create the CO<sub>2</sub> leakage pathway (it is assumed pre-existing leakage pathways are handled in a separate assessment). Once a pathway exists, however, buoyancy can allow mobile CO<sub>2</sub> leakage to continue even without overpressure. The damage component of scenario four can therefore extend indefinitely. Residual or mineral trapping, fault healing, geochemical mechanisms, or active mitigation may then be needed to

limit impacts. Recent research has focused on a number of intervention strategies that can be used to stop ongoing leaks in a relatively short time frame, assuming they are detected (Réveillère, 2012).

The sophistication of the risk assessment should depend on the available monitoring and characterization data. Without data, there is little justification for spending time and money on a complicated analysis. In early stages of a project—particularly pre-injection—data limitations can make overly detailed assessments ill-constrained and inaccurate. As a result, analyses must be continuously updated and improved as new information comes in. For the same reason, the monitoring and operation plans should evolve as well. This adaptive approach ensures that project resources can be properly allocated to minimize risk, while not wasting time and budget on extraneous efforts.

Table 3 describes the details of a phased approach to risk management. The plan is divided into three components: (a) monitoring and characterization, (b) modeling and analysis, and (c) operations and management. The tasks to be performed under each category change from one phase to the next, with a general increase in complexity and sophistication over time. The last phase (mitigation) represents contingency plans in case unexpected seismicity should occur—that is, either unacceptable events occur or new data suggest a higher seismic risk than originally estimated.

While it is important for a project to develop mitigation and remediation plans in advance and be ready to act upon them quickly, they may never be put into practice. A quick response to unfolding events, however, is an important aspect of risk management. While not all seismic events can be anticipated, speedy collection and interpretation of data, followed by immediate action, can lower the likelihood of severe or irreparable damage taking place.

**Table 3: Summary description of an induced seismicity risk management plan**

	Monitoring & Characterization	Modeling & Analysis	Operations & Management
Site-screening	<ul style="list-style-type: none"> <li>Collect regional stress estimates</li> <li>Collect regional seismicity observations</li> <li>Collect regional fault characterization</li> </ul>	<ul style="list-style-type: none"> <li>Back-of-the-envelope evaluations</li> <li>Identify red-flag site characteristics</li> <li>Identify sensitive infrastructure</li> </ul>	<ul style="list-style-type: none"> <li>Screen-out high risk sites</li> <li>Choose best site to balance seismic risk and other priorities</li> </ul>
Pre-injection	<ul style="list-style-type: none"> <li>Perform baseline 3-D seismic survey</li> <li>Identify faults and other structures</li> <li>Assess seismic resolution and fault visibility limits</li> <li>Drill characterization well(s)</li> <li>Measure (estimate) in situ stress</li> <li>Deploy limited microseismic array</li> </ul>	<ul style="list-style-type: none"> <li>Estimate overpressure buildup and maximum plume extents</li> <li>Perform reactivation analysis for observed faults</li> <li>Estimate likely <math>M_{max}</math> from unknown fault</li> <li>Develop baseline seismic hazard analysis</li> </ul>	<ul style="list-style-type: none"> <li>Alter operations strategy to address any newly identified concerns</li> <li>Select appropriate traffic-light thresholds or other triggers for action</li> <li>Engage with local community on potential seismic impacts and mitigation plans</li> </ul>
Injection & PISC	<ul style="list-style-type: none"> <li>Monitoring microseismicity</li> <li>Monitor above-zone pressure</li> <li>Monitor aquifer water-quality</li> <li>Perform regular falloff and other well tests</li> </ul>	<ul style="list-style-type: none"> <li>Frequently update seismic hazard analysis</li> <li>Analyze measured seismicity for statistical changes, correlation with pressure fluctuations, indications of previously unobserved faults, and indications of out-of-zone fluid migration</li> </ul>	<ul style="list-style-type: none"> <li>Implement traffic-light or similar seismicity reaction scheme</li> <li>Ensure timely collection, analysis, and interpretation of monitoring data</li> <li>Frequently re-evaluate quality and sensitivity of the monitoring plan</li> </ul>
If problematic seismicity occurs	<ul style="list-style-type: none"> <li>Quickly deploy additional surface geophones targeted at problem areas</li> <li>Consider additional downhole geophone deployment</li> <li>Performed controlled injection tests to probe seismic behavior</li> </ul>	<ul style="list-style-type: none"> <li>Implement full probabilistic risk analysis for high-priority infrastructure, critical water resources, etc.</li> </ul>	<ul style="list-style-type: none"> <li>Reduce, halt, or backflow injection</li> <li>Update local community on situation and ongoing operations</li> <li>Implement damage remediation and reimbursement plans, if necessary</li> <li>Evaluate major strategy changes, such as alternate injection locations or active pressure management</li> </ul>

## 3.2 PROBABILISTIC SEISMIC RISK ASSESSMENT

A methodology can be developed for quantifying ground motion hazards and risks by adapting the standard PSRA approach that is widely used to estimate the risk of structural damage from naturally occurring tectonic earthquakes. PSRA involves coupling the probability of an event occurring with its societal consequences, and it is generally carried out using the following procedure:

1. *Source Characterization*: Identify seismic sources, which may be individual faults or zones within which earthquake occurrence is assumed to be homogeneous
2. *Earthquake Occurrence Rate*: Estimate the average frequencies of occurrence of earthquakes of different magnitudes for each source
3. *Ground Motion*: Calculate the ground shaking resulting from earthquakes on each source at sites of interest. Ground shaking measures generally include ground velocity and acceleration at specified frequencies or seismic intensity, which are functions primarily of source magnitude and source-to-site distance.
4. *Hazard*: Derive a hazard curve representing the forecast annual probability of exceeding each ground motion value by integrating the frequencies of occurrence of ground motions generated by all sources. In conventional PSRA, hazard constitutes a long-term forecast, typically over time periods of several decades. For induced seismicity, the hazard has an inherent time-dependency.
5. *Vulnerability*: Develop a vulnerability function for each receptor (i.e. buildings, infrastructure, community population) that expresses the probability of creating a certain level of damage for a given ground motion value. Usually this involves structural analysis for buildings, or surveys asking people how they respond to given levels of shaking.
6. *Risk*: Derive a risk curve representing the annual probability of a given consequence, such as a specified degree of structural damage. This is accomplished by multiplying the hazard curve with the vulnerability function.

Steps 1 to 4 constitute a PSHA, while Steps 5 and 6 add the damage component necessary for risk evaluation.

While widely used for natural seismic hazards, standard PSHA and PSRA analyses require a number of modifications before they can be applied to induced seismicity. The next few sections address some of these limitations and methods for dealing with them.

### 3.2.1 Source Characterization

Three general types of sources are considered for PSHA:

1. *Known, generally larger faults*. These are characterized by defining their dimensions, geometries, faulting styles, slip rates, and ages of most recent activity. The maximum size earthquake that each is capable of generating is governed primarily by its area.
2. *Smaller (sub-seismic) unknown faults*. These can be characterized by a stochastic distribution of fault locations, sizes, orientations and slip rates determined by geostatistical simulation—e.g. Wen and Sinding-Larsen (1997)—constrained by geological and well data and the local tectonic setting.

3. *Crustal volumes within which the seismicity is not assigned to defined faults but is assumed to be uniformly distributed in space and has homogenous frequency-magnitude characteristics.* In conventional PSHA, definition of these source zones is based on a catalog of past seismicity.

### **3.2.2 Frequency of Occurrence**

There are two obstacles to applying the conventional treatment of earthquake occurrence to induced seismicity hazards. The first is that in conventional PSHA, the occurrence rates in Step 2 above are estimated empirically from the record of past seismicity in the region by applying the (modified) Gutenberg-Richter relationship described in Section 2.5.1. While empirical analysis of the induced earthquake catalog compiled by seismic monitoring can be applied to estimate site-specific frequency-magnitude statistics once injection is underway, no empirical database is available for pre-injection PSHA.

The second limitation of the conventional approach is that earthquakes occurring on any source are assumed to be independent events that happen randomly in time at the mean long-term rates given by the Gutenberg-Richter distribution; i.e. event probabilities within any time interval are given by a stationary Poisson distribution and are thus independent of time (Budnitz et al., 1997; Cornell, 1968). This means that the probability of an event depends only on the mean rate and not on any current information, such as the time of occurrence of the last event. Each of the earthquake sources is further assumed to be spatially homogeneous, which means that an event hypocenter is equally likely to be located at any point on the source.

These Poisson assumptions run counter to the generally accepted notion of the earthquake cycle as a stress renewal process, in which event probabilities should depend on the current state of the system, and in particular the time elapsed since the last event—e.g. Working Group on California Earthquake Probabilities (2003). They are, however, generally adopted for long-term (typically decades) occurrence forecasting and PSHA because—except for large characteristic earthquakes on a handful of the best characterized faults—insufficient information exists to constrain even the simplest time-dependent renewal models (Working Group on California Earthquake Probabilities, 2003). These simple models are inappropriate for describing fluid-induced seismicity sequences in which the strongest time and space dependence derives from the evolution of the fluid pressure field, rather than stress renewal under steady tectonic loading.

The assumption that earthquakes are independent events is also recognized as a significant limitation in conventional PSHA. Static and dynamic stress changes (and possibly other processes) in the volume of crust surrounding an earthquake can trigger daughter events, resulting in ubiquitous time- and space-clustering in observed seismicity, the most obvious manifestations of which are foreshock–mainshock–aftershock sequences. Indeed, aftershocks, including events that generate significant ground motion, are routinely removed from earthquake catalogs used in conventional PSHA precisely because they violate the Poisson assumptions. Modifications to time-independent hazard maps that take into account the short-term time dependence in earthquake frequency resulting from aftershocks have been calculated routinely on a 24-hour basis for California since 2005 (Gerstenberger et al., 2005). These short-term forecasts are estimated using the STEP procedure discussed in Section 2.5.3. Empirical approaches to induced earthquake PSHA using adaptations of the aftershock models described are discussed in the following section.

## **Empirical Analysis of Induced Earthquake Frequency-Magnitude Distributions**

An induced seismicity catalog compiled from microseismic monitoring during and after injection can be used for empirically-based occurrence forecasting that accounts for the non-stationary occurrence characteristics of induced seismicity in time and space. Most of the recent developments in empirical PSHA methods have been for application to short-term fluid injection to create enhanced geothermal reservoirs. A retrospective risk analysis for the 2006 stimulation of the Basel EGS (Baisch et al., 2009) considered only the increase in hazard over the background due to tectonic earthquakes for the entire 12-day period of injection and 30 years after shut-in. They employed a time-independent Poisson model based on the average occurrence rates derived from the complete catalogs for both periods, so that their approach is not predictive and could not be employed to estimate short-term hazard.

Current real-time monitoring protocols do not include hazard and risk estimates. Most EGS operators use a traffic-light system, originally developed for the Berlin geothermal project in El Salvador (Bommer et al., 2006), adapted to their site. This system generally incorporates four stages and is based on public response, maximum observed magnitude, and measured peak ground velocity. According to those three components, the injection will be either: 1) continued as planned (green); 2) continued but without increasing the rate (yellow); 3) stopped and pressure bleed-off started (orange); or 4) stopped with bleed-off to minimum wellhead pressure (red). The traffic-light system is defined ad-hoc and is mainly based on expert judgment. In the Basel, Switzerland EGS project, this system was not successful. The orange stage was triggered after an ML2.7 event, but reduction and the eventual shut-down of the injection did not prevent a magnitude ML3.4 later on the same day.

The objective of more recent development of empirical time-dependent methods by Bachmann et al. (2011) and Mena et al. (2013) has been to provide short-term (hours to days) seismicity rate forecasts and hazard estimates that are regularly updated by analysis of the seismicity on a near-real time basis, which can provide the basis for risk-based decision making and mitigation strategies. These methods are based on the aftershock models and the physics-based model of Shapiro et al. (2007, 2010) described in Section 2.5.3. The approach is to adjust the model parameters to fit the seismicity rates observed over an interval that increases with elapsed time by increments of equal length and ends at the current time. The updated model is then applied to forecast occurrence rates over a short time window in the immediate future. Therefore, the approach incorporates time dependence at two scales; the length of the time interval over which the parameters are held piecewise constant, and within each interval the time dependence inherent in the models.

The Reasenber and Jones (1989) model underlying the STEP procedure has no provision for dealing with non-stationary, time-dependent forcing from injection-induced pressure changes, and so is not appropriate for describing induced seismicity. The ETAS model as modified by Bachmann et al. (2011) embodies both interaction triggering and events induced by time-varying injection according to a simple linear dependence of occurrence frequency on injection flow rate. Using formal statistical evaluations of forecast rates against the seismicity (see <http://cseptest.org>) observed at the Basel EGS project, Bachmann et al. (2011) and Mena et al. (2013) found that the rates forecast using the modified ETAS model within 6-hour time windows provided acceptable overall fits to the observed seismicity when all the parameters except the  $b$ -value were allowed to vary in the fitting process (i.e. six free parameters from a total of seven). They then used the forecast occurrence rates to calculate the hazard in each 6-

hour window using the conventional method and regional ground motion prediction equations (see below). It should be noted that even if there are tradeoffs in fitting the relatively large numbers of free parameters, all that is required is that relationship provides an acceptable estimate of seismicity rates during the next time interval.

Mena et al. (2013) extended the results of Bachmann et al. (2011) by comparing the performance of the Shapiro model with two ETAS models. They found that the Shapiro model performed somewhat better overall than ETAS when just the  $b$ -value or both  $b$  and  $\Sigma$  were treated as free parameters, but the ETAS models performed slightly better in predicting the number of larger ( $M > 2$ ) events within each 6-hour window. It is significant that the Shapiro model performed poorly when fixed generic parameters taken from Shapiro et al. (2010) were used. This suggests that, as might be expected, model parameters are not portable, and that application of the models for PSHA must be on a site-specific basis.

The ML3.4 maximum magnitude event of the Basel sequence occurred 6 hours after the well was shut in. The probability of  $M > 3$  events during this time window estimated by all of the models was only about 15%, compared with about 45% at the time of the previous larger ( $M 2.7$ ) event during active injection before shut-in. The probability of exceeding the EMS (European Macroseismic Scale) Intensity V actually produced by the maximum event was calculated as about 5%.

Occurrence rates computed using the modified ETAS and Shapiro models both depend on injection flow rate rather than pressure, the parameter operative in reducing fault effective stress. While the flow rate is the parameter that can be adjusted directly during injection operations, for example to effect mitigation measures, its relationship to wellhead and downhole pressure is not always straightforward. For example, the injection rate into the Paradox Valley well has been held more or less constant for the past 13 years but the wellhead pressure has gradually increased, indicating reducing injectivity (proportional to the ratio of injection rate to pressure). However, preliminary results obtained by Bachmann suggest that for the particular case of Paradox Valley the forecasting performance of ETAS appears essentially the same when either pressure or rate is used as the independent variable.

In addition to demonstrating the performance of the ETAS and Shapiro models in forecasting rates over short (several hours) time windows, Mena et al. (2013) evaluated their performances over longer time horizons. They found that for the Basel injection the performances of both models over a forecast interval of 15 days (i.e. including both the injection and post-injection periods) progressively improved as the learning period used to estimate the parameters was increased from 1 to 4 days, when the performance measures for each model approach those achieved over 6-hour forecast intervals. This implies that the state of the system undergoing injection at an increasing rate did not change significantly on a time scale of weeks.

The question remains, however, to what extent this kind of procedure scales to the much longer times over which GCS injection and post-shut-in performance assessment take place. The maximum length of a valid forecast window is governed by the time scale of the dynamic processes operating in the reservoir, which could include, for example, changes in permeability resulting from slip and deformation or geochemical reactions. On the other hand the learning time must be long enough to collect a large enough seismicity sample from which to derive a valid representation of the quasi-stationary state of the system over the forecast window. Recent work applying the Shapiro model to the 22 year-long injection history and seismicity record from

the U.S. Bureau of Reclamation (USBR) deep brine disposal well in Paradox Valley, Colorado (Ake et al., 2005) shows that it performs very poorly over long time windows, especially when the injection rate is not monotonically increasing.

The alternative models considered by Bachmann et al. (2011) and Mena et al. (2013) represent epistemic uncertainty in the PSHA input. Following the conventional approach, the alternative models can be weighted and treated as weighted branches of a logic tree or by a Monte Carlo method. While the model weights are commonly estimated using expert opinion, Mena et al. propose an objective and ostensibly more rigorous approach using Akaike weights (e.g. Wiemer et al. (2009)). The weights are computed and assigned based on the relative likelihoods of the models within each forecast window, and so are time-dependent.

All of the recently developed approaches to time-dependent PSHA for induced seismicity retain the assumption of homogeneous Poisson spatial occurrence within the crustal volume influenced by the injection. However, as discussed in Section 2.5.3, Bachmann et al. (2012) showed that  $b$ -values computed for the Basel sequence are spatially variable. They propose that this is probably a result of decreasing fluid pressures away from the injection interval, and that it implies that the probability of larger events increases with distance and time. At the short distances often applicable in calculating ground motion from induced seismicity, especially for assessing nuisance risk, localization of earthquake source zones assumes greater importance. Therefore, future developments of empirically-based PSHA methods should ideally consider the spatial evolution of the seismicity distribution in hazard updating schemes like those developed by Bachmann et al. (2011) and Mena et al. (2013).

Source localization is particularly important in the treatment of discrete fault sources, which may have been identified during site characterization or may be revealed by the induced seismicity itself, as in the case of some sequences induced by waste water injection (e.g. Keranen et al., 2013). In the latter case, a fault source could be defined and characterized following the procedure used in routine STEP aftershock analysis (Gerstenberger et al., 2004). In the case of these presumably larger faults the ground motion at close distances depends on finite fault (as opposed to point source) effects such as the direction of rupture (see Section 3.2.2). In addition, the maximum possible magnitude on that fault can be estimated if its dimensions are known.

The maximum magnitude ( $M_{\max}$ ) at which frequency–magnitude distributions are truncated has a significant influence on the hazard at higher ground motion levels (e.g. Bachmann et al., 2011), but selection of  $M_{\max}$  based on the data usually available remains a challenge. Certainly, if faults favorably oriented for failure have been identified within or intersecting the volume likely to be affected by pore pressure perturbations, then  $M_{\max}$  can be estimated from the dimensions of the largest of those. Failing that, Shapiro et al. (2011) (see also Mena et al., 2013) have proposed that the magnitude of the largest expected event can be empirically related to the dimensions of the pressure-perturbed volume, which can be approximated by the cloud of induced seismicity. The assumption underlying their physical model to explain the observations is that the maximum magnitude earthquake occurs on a (undetected) fault having dimensions approximately equal to the dimensions of the perturbed volume and that is largely contained within the volume. However, this also implicitly assumes that undetected faults of all sizes up to the dimension of the pressurized volume are pervasive in the vicinity of the injection well, and some are favorably oriented for slip. Therefore, since presumably that will not always be the case, it would perhaps be more accurate to say that the model places an upper bound on  $M_{\max}$ . On the other hand, their explanation discounts the possibility that failure of only a small patch of a fault within a pressure

plume can result in a rupture that continues to propagate across the fault outside the plume, leading to an event larger than the inferred  $M_{\max}$ . Also based on observations, McGarr (2014) has proposed a simple relationship between the upper bound magnitude and seismic moment and the net cumulative volume of injected fluid, but does not regard it as giving an absolute physical limit.

It is frequently observed that the largest events occur after fluid injection has been shut off (Baisch et al., 2010; Deichmann and Giardini, 2009), but so far there has been little work to investigate this. Baisch et al. (2010) attribute larger events after shut-in to overpressures that continue to increase, but have less steep gradients than during injection. In their numerical model they find that neighboring fault patches are similarly stressed and thus it is easier for slip that initiates on one patch to propagate to the others. Bachmann et al. (2012) and Goertz-Allmann and Wiemer (2012) analyzed the probabilities of large magnitude events in more detail using geomechanical modeling of the Basel injection. They found that the probabilities of large magnitude events increase after shut-in if the  $b$ -value varies spatially and temporally.

### **Physics-Based Simulation of Induced Earthquake Occurrence**

The empirical methods described in the last section rely on the compilation of a catalog of induced seismicity during the injection and post-shut in phases of a project. However, reliable long-term hazard and risk estimation for planning and regulatory purposes before injection begins presently remains an unsolved problem. As demonstrated by Bachmann et al. (2011) and Mena et al. (2013) site-specific parameters are required for reliable application of empirical models. It may be feasible in some cases to conduct a pilot injection to constrain preliminary estimates of the parameters that could be used during the initial stage of a project, but such an operation would be expensive.

Physics-based simulation of time-dependent frequency-magnitude behavior offers one possible solution to this problem. Numerical simulation has been used to investigate induced seismicity at enhanced geothermal (e.g. Baisch et al. 2009, 2010; McClure and Horne, 2011) and CO<sub>2</sub> sites (e.g. Cappa and Rutqvist, 2012; Rinaldi et al., 2014). These modeling approaches have been carried to varying levels of sophistication, but all involve hydro-mechanical modeling to simulate overpressures that can induce failure on model elements according to some implementation of the Mohr-Coulomb law. However, none has yet been applied directly to generate frequency-magnitude distributions for PSHA.

Baisch et al. (2009, 2010) employed a finite element implementation of a coupled hydro-mechanical model to simulate induced earthquake sequences on single faults. They use a highly simplified model in which Mohr-Coulomb shear failure occurs abruptly with a constant prescribed stress drop. Upon the failure of an element, stress is transferred to nearest-neighbor elements according to fixed percentages, thus allowing the potential for those elements to fail to produce cascades representing larger events. While this model is computationally efficient and could be used to generate entire earthquake sequences as PSHA input, it is probably too simplified to represent important aspects of the earthquake process. In contrast, the model of McClure and Horne (2011) incorporates a rate-and-state frictional law that captures critical features of the entire earthquake cycle, but is computationally intensive and so far has only been applied to 1-D (line) faults embedded in a 2-D medium. The coupled hydro-mechanical approach of Cappa and Rutqvist (2012) and Rinaldi et al. (2014) utilizes 3-D flow modeling and a relatively simple slip-weakening frictional law. Unlike the other techniques, their geomechanical

model is fully elastodynamic, which provides a more complete description of dynamic earthquake rupture and includes wave propagation in the surrounding medium from which ground motions are calculated directly. This approach is also too expensive computationally to be used to generate full seismicity catalogs.

Various simulation approaches have been developed for forecasting the occurrence of larger earthquakes in California, as described, in a dedicated issue of *Seismological Research Letters* (v. 83, November/December, 2012), and a large-scale effort is underway to apply these methods to PSHA (J. Dieterich, personal communication, 2013). The National Risk Assessment Partnership (NRAP) is currently implementing a physics-based approach to generating seismicity catalogs for pre-injection PSHA (Foxall et al., 2013) by adapting one of these methods—the code RSQSim (Dieterich and Richards-Dinger, 2010; Richards-Dinger and Dieterich, 2012)—to incorporate a time-varying overpressure field.

RSQSim utilizes an empirical rate-and-state law derived from laboratory experiments in which the frictional coefficient on each fault patch at a given time depends on the current slip velocity and state of the patch. The variable describing the state evolves over time, and in the rate-and-state law used in RSQSim, it is interpreted as the average lifetime of the asperities at which the two sides of the fault are in contact. Rate-and-state frictional laws provide the most complete description of the entire earthquake cycle currently available (e.g. Ben-Zion, 2008). The key feature of RSQSim that enables rapid simulation of very large seismicity catalogs over arbitrarily long time periods is that time steps are determined adaptively by approximate analytical calculations.

Faults and fractures in the simulation model are gridded into elements and are subject to constant-rate long-term tectonic shear loading. A time-dependent overpressure field applied to the faults is computed in advance by a separate flow simulation driven by a pre-defined injection scenario. Therefore, unlike the methods described above, evolving fault permeability is not directly coupled to fault slip. An induced earthquake nucleates when the overpressure on one of the elements causes its frictional strength (at the current value of the time-varying friction coefficient) to drop below the shear stress. The stress release resulting from the slip of the element is transferred to all of the other elements in the model, which can cause some of them also to fail. In this way larger earthquakes are produced by cascading sequences of element failures, or sub-events. The nucleation times, slip durations and stress drops of all the sub-events that comprise each earthquake in the simulated seismicity catalog are used directly to calculate ground motions, as described in the following section. One important limitation of RSQSim is that fault slip is quasi-static, so that elastodynamic effects can only be approximated.

Input parameters for the simulations generally fall into two classes: those that potentially can be constrained by site investigations, and generic parameters from previous studies. The first class includes fault/fracture characteristics, material properties, the in situ tectonic stress field, fault slip rates, and reservoir and fault flow parameters. The second includes rate-and-state and other parameters used in RSQSim.

The scaling of rate-and-state parameters from laboratory to field is the topic of vigorous research, so these parameters are subject to considerable epistemic and aleatory uncertainty. An important component of the NRAP work is calibration of these parameters by comparing temporal and spatial occurrence statistics of simulated catalogs with observed induced seismicity at well-characterized sites like the USBR Paradox Valley project. The degree of uncertainty in

potentially field-measurable parameters depends on the specific site conditions and the scope and thoroughness of site characterization studies. These uncertainties are dealt with in PSHA calculations by generating a large number of realizations that sample from epistemic and aleatory distributions on the parameters using Monte Carlo and/or logic tree approaches.

### **3.2.3 Ground Motion**

A major difference between PSHA for induced and naturally-occurring seismicity is the need to calculate ground motions from small induced events that do not pose a risk of structural damage, but can be strongly felt at short distances. Depending on the distance to nearby communities, magnitudes as low as M1.5–M2 may need to be included in the hazard analysis.

Conventional PSHA employs empirical ground motion prediction equations (GMPEs) derived by regressions on worldwide strong motion data (e.g. Abrahamson and Shedlock, 1997). Existing GMPEs do not extend to magnitudes below M4.5–M5, and even then are very poorly constrained for the smallest events and short distances (e.g. Bommer et al., 2006). Douglas et al. (2013) recently developed GMPEs specifically for magnitudes less than M3.5 and short distances, based on data from six geothermal areas. The aleatory uncertainties on the generic empirical GMPEs derived from the data are large, primarily owing to site-to-site variability, and could lead to bias in calculated ground motions. Therefore, Douglas et al. (2013) regard a set of 36 stochastic GMPE models also derived from the data as representing empirical uncertainty, and recommend treating these models as branches of a logic tree weighted using site-specific information, including local recordings.

The results of Douglas et al. (2013) highlight the need to use site-specific data in estimating local ground motions from induced earthquakes. In addition to constraining weights for the Douglas et al. (2013) stochastic models, these data can also be used to develop local empirical relations (e.g. Convertito et al., 2012) or to modify existing ones (Bommer et al., 2006).

Microearthquake seismograms from small earthquakes can also be used as empirical Green's functions (EGFs) for site-specific, physics-based synthesis of ground motion from larger events (e.g. Hutchings et al., 2007; Hutchings and Wu, 1990). The EGFs contain complete information about the point-source response (wave propagation) of the Earth along specific source-site paths. Larger events are modeled as a composite sequence of point-source sub-events on the fault plane that propagates at the earthquake rupture velocity. The ground motions at specific sites are calculated by convolving each point-source with the appropriate EGFs and summing the in-phase contributions from all of the sub-events. Most ground motion calculation approaches to date have employed a kinematic description of the rupture process in which the sub-event parameters and rupture velocity are prescribed a priori (e.g. Hartzell et al., 1999; Hutchings et al., 2007). A few more recent studies have used spontaneous dynamic (Hartzell et al., 2005) or dynamically-constrained (Pulido and Dalguer, 2009) rupture models. In the NRAP methodology, sub-event parameters (slip, rise time, stress drop) are passed directly from the RSQSim simulations described in Section 3.2.2.1. The rupture velocity is described naturally by the timing of successive sub-events.

Prior to injection, when in most cases microearthquake recordings that can be used as EGFs will not be available, it may often be feasible to use synthetic Green's functions. These are calculated by modeling wave propagation from an array of point sources within the likely source volume and on identified faults through the local seismic velocity and attenuation structure. The accuracy

of the latter will depend on the amount of data available from site and regional characterization, including local recording of background earthquakes, borehole vertical seismic profiles, velocity and density logs and stratigraphy, and local and regional geology. One method of deriving Green's functions and crustal velocity structures without discrete sources is ambient noise tomography, which has recently been applied at local scales (Matzel, 2012).

Given the velocity and attenuation structures, the Green's functions are synthesized using either a numerical (e.g. Graves, 1996) or analytical (e.g. Hartzell et al., 1999) wave propagation method. Depending on the overall scale of the problem, numerical wave propagation modeling using finite difference codes is generally practicable only at frequencies less than 1–2 Hz. Analytical methods are much more computationally efficient, but are generally limited to 1-D layered structures. As an example, synthetic Green's functions used in the development of the NRAP PSHA methodology are calculated using the analytical frequency-wavenumber code of Saikia (1994).

Green's function calculations suffer from lack of site-specific information at high wavenumbers (small scales). Therefore, hybrid techniques that employ finite difference at lower frequencies and EGFs (McCallen et al., 2006) or semi-stochastic approaches (Graves and Pitarka, 2010) at higher frequencies have been employed. Semi-stochastic methods such as that developed by Boore (2003) are based on observations that source radiation and wave propagation tend to become stochastic at frequencies above 1 Hz.

Ground acceleration and velocity amplitudes at a specific receiver site are strongly influenced by amplification effects that depend on the characteristics of the near-surface geology.

Conventionally, amplification factors are applied to bedrock ground motions based on broad site classifications, often parameterized in terms of the S-wave velocity at a depth of 30 meters (VS30). Recently, inversion methods have been developed to obtain site response spectral amplifications as a function frequency from ambient noise recordings (Herak, 2008) and near-surface velocity profiles (Scherbaum et al., 2003). One approach is to use near-surface-velocity profiles to calculate analytic Green's functions which are then convolved with site response functions to obtain site-specific Green's functions (Scognamiglio and Hutchings, 2009).

### **3.2.4 Vulnerability**

The effects of ground-motion produced by medium to large earthquakes ( $M_w > 4.5$ ) on structures are usually modeled with a fragility function that expresses the probability of structural damage as a function of ground-motion intensity. These are combined with hazard curves to calculate damage risk; *i.e.* the probability of exceeding given damage levels at a site over a specified time period. Standard functions can be applied to assess structural damage from induced earthquakes, and extensive literature on this topic is available (e.g. FEMA, 2013). However, an equivalent methodology has not yet been published to address the risk of nuisance and the attendant impact on public perception caused by seismicity induced by fluid injection and other anthropomorphic activities.

The effects of felt but non-damaging ground motions have been extensively studied in the context of vibrations generated by mining and construction, which has led to the development of national (American National Standards Institute) and international (International Standards Organization) standards in the form of deterministic acceptability criteria (Dowding, 1996). These criteria formed the basis for the development by the U.S. DOE of a protocol and

recommended best practices for assessing and mitigating risks associated with ground motions induced by EGS (Majer et al., 2012a,b). The DOE guidelines can also generally be applied to potential GCS-induced seismicity. Therefore, following the recommendations in the guidelines, nuisance fragility functions that can be used to estimate risk from hazard curves are being developed as part of the NRAP PSRA methodology, as described in Foxall et al. (2015). Based on the definition of nuisance risk as the probability that an individual will not find the seismic environment acceptable, the same general approach followed by Federal Emergency Management Agency (FEMA, 2013) for damage fragility is applied to model the response of individuals to ground-motion. The deterministic acceptability criteria considered in Majer et al. (2012a,b) are then used to anchor human response fragility functions. Currently, development of the nuisance fragility functions is based on peak acceleration as the ground motion metric, but future work will investigate other parameters such as velocity or spectral estimates to determine which is the most appropriate for measuring human response.

### 3.3 PROBABILISTIC LEAKAGE RISK ASSESSMENT

A parallel methodology to PSRA, a Probabilistic Leakage Risk Assessment (PLRA), can be developed to address leakage risks. The basic steps to develop a PLRA follow the same structure as the PSRA approach:

1. *Source Characterization and Frequency of Occurrence*: Identify faults and estimate the average frequencies of occurrence of earthquakes of different magnitudes as a result of injection. This step is nearly identical to the previous PSRA analysis, and faces the same challenges: The major difference is that only faults that penetrate hydrologic seals are included in the analysis, as only these can lead to leakage. For CO<sub>2</sub> leakage assessment, only faults that intersect the mobile CO<sub>2</sub> plume are included.
2. *Leakage*: Estimate the leakage rate along a given fault as a result of induced slip. This rate will depend on the fault properties, brine and CO<sub>2</sub> properties, caprock structure, reservoir pressures and saturations, and other hydrologic factors. Typically this will involve using a reservoir simulator to model the leakage behavior along individual faults, accounting for significant uncertainties in permeability and other properties. Analytical or semi-analytical approximations for leakage along a fault can also be used. Reduced-order models for these systems may also be useful.
3. *Hazard*: Derive a hazard curve representing the probability of exceeding a certain leakage volume in the time period of interest by integrating the leakage generated by all sources.
4. *Vulnerability*: Develop a vulnerability function for each receptor (i.e. a drinking water aquifer) that expresses the probability of creating a certain level of impact for a given leakage rate and/or volume. This vulnerability function can be developed using empirical experience or derived from simulations of the aquifer system when a given volume of contaminants is introduced.
5. *Risk*: Derive a risk curve representing the probability of a given consequence—such as a total volume of water exceeding a maximum concentration limit—by convolving the hazard curve with the vulnerability function.

Due to the physics of the process, there are important time- and space-dependencies that may enter the analysis. For example, the brine and CO<sub>2</sub> leakage rates are tightly tied to reservoir

pressure and saturation and their evolution over time. Also, operator intervention and mitigation if a leak does occur may factor into the analysis. Some simplifying but conservative assumptions can be included to address these issues. Alternatively, simulation techniques can be used to capture these complexities directly.

The physics of fault leakage are quite complicated, and simulation tools are useful for understanding the fate of brine and CO<sub>2</sub> if a permeable pathway is created. At the same time, very large uncertainties in the structure and properties of the storage system exist. Therefore, the results of any one simulation should be viewed with caution, and efforts should be made to understand the sensitivity of the results to different assumptions. In general, the goal is not a perfect prediction of how the system will behave. Rather, all one really needs for risk management purposes is order-of-magnitude estimates of potential leakage rates and impacted volumes.

### **3.3.1 Source Characterization and Earthquake Recurrence Rates**

This step can be performed in tandem with the PSRA analysis, as the objectives are identical. The methods and caveats described in Sections 3.2.1 and 3.2.2 continue to apply. For a leakage assessment, however, the focus is limited to the subset of faults that penetrate hydrologic seals. Again, two fault populations need to be considered: known faults and a distribution of unknown (sub-seismic) faults. Depending on the thickness of the seals and the resolution of the baseline 3-D seismic survey, the latter population may or may not be a concern. Ideally, the operator would be able to establish with confidence that all faults sufficiently large to penetrate hydrologic seals are visible in a baseline seismic survey. Given the inherent challenges in identifying faults described earlier, however, such a determination may not be possible. If not, geostatistical techniques can be used to parameterize a distribution of smaller faults and include them into the leakage analysis. For example Jordan et al. (2011) present a statistical strategy for estimating the likelihood that the pressure and/or CO<sub>2</sub> may come in contact with smaller faults.

CO<sub>2</sub> storage sites often rely on multiple sealing layers. At some sites, a single, larger fault may penetrate all layers and form a direct leakage pathway to a sensitive aquifer. Such direct pathways are a top concern. Multiple, smaller faults at different depths could potentially combine to create a complete leakage pathway. Complex pathways would likely lead to lower leakage volumes, but they remain a concern and should be considered.

Also, while PSRA is concerned with seismically active faults, the leakage assessment must also consider faults that are intrinsically permeable under in situ conditions, or faults that may be re-activated aseismically.

### **3.3.2 Leakage Hazard**

Given a distribution of leakage pathways, simulation techniques can be used to estimate leakage rates. Sufficient data usually exist to provide a rough forecast of the pressure and saturation distribution in the reservoir, and the reservoir model can be refined through history-matching of monitoring data as the operation proceeds. The central challenge in leakage analysis, however, comes in assigning permeability and flow properties to fault pathways, both before and after reactivation. As described in Section 2.3.3, some techniques are available to help guide this hydromechanical characterization, but large uncertainties will invariably persist. These uncertainties should not be under-estimated and must be reflected in a conservative analysis.

Several studies have developed fault leakage models of varying levels of complexity (e.g. Chang et al., 2009; Chen et al., 2013; Mazzoldi et al., 2012; Pruess, 2005; Zhang et al., 2010). A general observation is that higher-fidelity models invariably require significantly more computational expense. Given that many model realizations are required to adequately address system uncertainty, high-fidelity approaches can quickly become intractable except for those with access to significant super-computing resources. In light of this fact, cheap reduced-order models are appealing (e.g. Chang et al., 2009) perhaps supplemented by and/or calibrated to a few high-fidelity case studies.

NRAP has developed a framework for performing probabilistic leakage hazard assessments. The basic approach is to use high-fidelity simulations of various components of the GCS system (reservoir, faults, wellbores, aquifers) to calibrate simplified reduced-order models that approximate the full-physics behavior, but at significantly less computational expense. These computationally inexpensive sub-modules are then linked and applied within a Monte-Carlo framework to develop leakage hazard and risk curves, including the most important uncertainties in input parameters.

### **3.3.3 Vulnerability**

The vulnerability of an aquifer to brine and/or CO<sub>2</sub> contamination can be assessed using an understanding of the aquifer geochemistry and the likely leakage volumes. In practice, such an assessment can range from simple models to quite sophisticated reactive-transport modeling. The NRAP project has published a companion report on aquifer vulnerability issues, refer to (Carroll et al., 2016) for extensive details on this topic.

#### **4. RECOMMENDATIONS**

Based on the discussion above, a number of recommendations seem prudent for operators and regulators to consider:

1. *There are advantages to choosing sites in proximity to previous carbon storage or oil and gas developments.* A large part of the seismic risk stems from lack of knowledge about the subsurface at a given site. By locating new injection wells near previous development, characterization and monitoring efforts can often be leveraged. A number of large carbon storage pilot projects have been co-located with gas field developments—e.g. In Salah and Snøhvit (Eiken et al., 2011)—allowing for detailed and cost-effective characterization campaigns. Also, if a particular well has given no indications of seismicity problems, it is reasonable to expect that a new well sited nearby in the same formation would be low-risk as well under similar operational conditions. Of course, there is always a chance that they will exhibit very different behavior due to subsurface heterogeneity. It is also inevitable that many projects will be sited in greenfield areas, with very little prior knowledge.
2. *Obtain quality in situ stress estimates.* It is difficult to understand geomechanical behavior without reasonable estimates of the in situ stress. Well-established techniques exist for estimating the principal stress magnitudes and orientations from well tests and logging tools, and there are few reasons not to employ them in one or more wells at the site, other than cost. This work should explicitly include efforts to estimate the maximum horizontal stress, which is typically the most difficult to constrain in practice. Data from multiple tests can also give some indication of the stress uncertainty. While additional constraints on the in situ stress can be obtained from regional observations and earthquake focal mechanisms, the value of direct, local measurements cannot be overestimated.
3. *Attempt to estimate fault density statistics and the “largest unobserved fault.”* For a given seismic survey, there will be some threshold size fault that can go undetected. Faults below this threshold size constitute an important, but difficult-to-characterize contribution to seismic and leakage hazards. The ability to resolve faults with reflection seismic is typically determined by their offset. In some cases fault offsets may be empirically-related to fault length. The dimensions of the “largest unobserved fault” can be used to bound the maximum magnitude that may be experienced on an unknown source (e.g. Mazzoldi et al., 2012). Empirical observations of faulting also indicate that fault density and size distributions generally follow simple power-law relationships (e.g. Scholz, 2002), which is often cited as the underlying reason for Gutenberg-Richter earthquake recurrence statistics. An understanding of the faulting regime, regional faulting statistics, and other types of observations may therefore help constrain the likelihood of encountering a fault of a given size that is well-oriented for slip.
4. *Under-pressured reservoirs may pose lower risk.* One key advantage of injecting into depleted oil and gas fields is that the net fluid balance implies large overpressures can be avoided. This is not a panacea for the seismic hazard, but will reduce it significantly. Unfortunately, the storage capacity available in depleted reservoirs is relatively small. Several saline storage projects are considering co-production or pre-production of brine to achieve a similar effect. The excess brine may be disposed of in a shallower layer—

moving the induced seismicity concern to a shallower, brine-only layer—or it can be consumed in various industrial processes. Excess brine could also potentially be used for water-flood EOR in nearby fields.

5. *Resilient seals are crucial, including shallow seals.* While significant effort should be put into avoiding induced seismicity in the first place, it is pragmatic to choose sites that have multiple seals in case a larger seismic event were to occur. There is also an advantage to having widely-spaced seals, even if the total seal thickness is not all that great. A shallow seal close to protected groundwater and far above the injection horizon is less likely to be compromised by an earthquake event—even if the radial extent of the slip patch is several hundred meters. These shallow seals can therefore provide last-ditch barriers. Resilient sealing systems are also inherently useful regardless of the leakage mechanism: induced seismicity, hydraulic fracture, thermal fracture, pre-existing fractures, etc.
6. *Avoid downward pressure migration.* To date, site selection has been primarily based on the properties of the reservoir units and immediate caprocks. This is understandable, as reservoir performance and seal integrity are the top two concerns. Several waste-water injection analogs, however, have experienced the most significant seismic events on basement faults well below the injection interval. Deep, brittle basement faults are particularly susceptible to seismicity. It is therefore important for projects to consider how pressure might migrate *below* the reservoir interval, and to focus some characterization effort on deeper units. Unfortunately, basement faults are often poorly resolved on seismic surveys. Sealing units below the reservoir unit can help mitigate this concern.
7. *The ground motion hazard attenuates quickly with distance.* The ground motion experienced by a building (or person) strongly depends on the distance to the source. Sites in remote locations will automatically have a higher tolerance for seismicity than those near populated centers. Similarly, regions with strict seismic building codes will have lower vulnerability than regions without seismic design standards.
8. *Deploy microseismic monitoring arrays.* Arrays of seismometers having appropriate sensitivity and response characteristics should be included in the suite of monitoring techniques deployed at a GCS site. Shallow geophone wells are relatively cheap compared to other monitoring investments. That said, it is not a trivial cost. Because of budget constraints, a project might consider a phased deployment strategy, only installing a few stations prior to injection. A limited deployment can be used to assess the general level of seismicity, but will only provide crude location estimates. If concerning seismicity is detected as operations proceed, the project could then invest in additional wells providing improved areal coverage and hence more accurate event locations. As an intermediate solution, temporary surface arrays can often be deployed relatively quickly to supplement existing coverage. Like most field operations, it is common to encounter hiccups during installation and calibration of the seismic sensors and recorders. Plenty of time should be included in the project timeline for testing of the array. Deploying the array far in advance of injection also provides an opportunity to develop a reasonable baseline catalog.
9. *Collect and analyze data in a timely fashion.* Monitoring data are only useful once it is processed, interpreted, and in the hands of the operation manager. The ability to quickly

react to changing subsurface conditions is an important part of mitigation. Focused effort should be put into automating and streamlining the processing and analysis workflow for the whole suite of monitoring tools, and minimizing the time window from data collection to decision-ready interpretation.

10. *Consider a slow ramp up to target injection rates.* The largest uncertainty about surface behavior occurs as injection begins and pressure moves into an “unexplored” volume. While it is tempting to ramp up to maximum injection rates as quickly as possible, an operator might consider a slower, stepped buildup to the target rate/pressure. A low-rate injection can be used to send a weak pressure (and temperature) pulse out into the formation to see if any sub-seismic faults, fractures, or other hazards exist in the near wellbore region. The operator can also look for indications of a pressure threshold for inducing seismic events as the pressure is built up. The same strategy and analysis can also be used to look for indications of hydraulic fracturing. For operational and reservoir performance reasons, however, this buildup period would likely be kept fairly short (days or weeks) so this strategy is only useful for exploring the near wellbore region.
11. *Falloff testing.* Much like a build-up test, falloff testing is tremendously useful for looking for indications of fracturing, faults, and compartmentalization. Falloff analysis can also be used to look for changes in injectivity over time. Unfortunately, interpreting these tests is complicated by pressure/volume/temperature, wellbore storage, and multiphase challenges associated with supercritical CO<sub>2</sub>. Placing formation pressure and temperature gauges as close to the injection interval as possible is helpful for constraining the interpretation of the data.
12. *The monitoring and characterization plan should be driven by risk assessment needs.* A probabilistic risk assessment can reveal the impact of a given parameter’s uncertainty on risk. These sorts of analyses can therefore be used to assess the value of a given piece of information in lowering uncertainty and risk for the project, which is helpful to guide decisions about the monitoring and characterization plan.

*Experience with induced seismicity at carbon storage sites is limited to date, and best practices will likely evolve as field experience grows. While induced seismicity is a serious concern and should be carefully addressed by all future projects, evidence to date suggest that good site selection and careful project design can lower seismic risk to acceptably low levels.*

## 5. REFERENCES

- Abrahamson, N.; Shedlock, K. Overview. *Seismological Research Letters* **1997**, *68*, 9–23.
- Ake, J.; Mahrer, K.; O’Connell, D.; Block, L. Deep-injection and closely monitored induced seismicity at Paradox Valley, Colorado. *Bulletin of the Seismological Society of America* **2005**, *95*, 664–683.
- Amitrano, D. Brittle-ductile transition and associated seismicity: Experimental and numerical studies and relationship with the b value. *J. Geophys. Res. - Solid Earth* **2003**, *108*, B1.
- Amitrano, D. Variability in the power-law distributions of rupture events. *The European Physical Journal Special Topics* **2012**, *205*, 199–215.
- Bachmann, C. New approaches towards understanding and forecasting induced seismicity. PhD thesis, ETH Zurich, 2011.
- Bachmann, C.; Wiemer, S.; Goertz-Allmann, B.; Woessner, J. Influence of pore-pressure on the event-size distribution of induced earthquakes. *Geophysical Research Letters* **2012**, *39*.
- Bachmann, C.; Wiemer, S.; Woessner, J.; Hainzl, S. Statistical analysis of the induced Basel 2006 earthquake sequence: Introducing a probability-based monitoring approach for enhanced geothermal systems. *Geophys. J. Int.* **2011**, *186*, 793–807.
- Baisch, S.; Carbon, D.; Dannwolf, U.; Delacou, B.; Devaux, M.; Dunand, F.; Jung, R.; Koller, M.; Martin, C.; Sartori, M.; Secanell, R.; Voeroes, R. *Deep heat mining Basel—Seismic risk analysis*; Technical report; Serianex, 2009.
- Baisch, S.; Voeroes, R.; Rothert, E.; Stang, H.; Jung, R.; Schellschmidt, R. A numerical model for fluid injection induced seismicity at Soultz-sous-Forets. *International Journal of Rock Mechanics and Mining Sciences* **2010**, *47*, 405–413.
- Barton, N. The shear strength of rock and rock joints. *International Journal of Rock Mechanics and Mining Sciences & Geomechanics Abstracts* **1976**, *13*, 255–279.
- Benson, S.; Cook, P.; Anderson, J.; Bachu, S.; Nimir, H.; Basu, B.; Bradshaw, J.; Deguchi, G.; Gale, J.; von Goerne, G.; et al. *Underground geological storage*; IPCC Special Report on carbon dioxide capture and storage, 2005; p 195–276.
- Ben-Zion, Y. Collective behavior of earthquakes and faults: Continuum-discrete transitions, progressive evolutionary changes, and different dynamic regimes. *Reviews of Geophysics* **2008**, *46*, RG4006.
- Bommer, J. J.; Oates, S.; Cepeda, J. M.; Lindholm, C.; Bird, J.; Torres, R.; Marroquin, G.; Rivas, J. Control of hazard due to seismicity induced by a hot fractured rock geothermal project. *Engineering Geology* **2006**, *83*, 287–306.
- Boore, D. Simulation of ground motion using the stochastic method. *Pure and Applied Geophysics* **2003**, *160*, 635–676.
- Bourdet, D. *Well Test Analysis: The Use of Advanced Interpretation Models*; Elsevier, Amsterdam, 2002.
- Budnitz, R.; Apostolakis, G.; Boore, D.; Cluff, L.; Coppersmith, K.; Morris, P. *Recommendations for probabilistic seismic hazard analysis: Guidance on uncertainty and the use of experts, v1.*; Technical Report NUREG/CR-6372, US NRC; 1997.

- Cappa, F.; Rutqvist, J. Seismic rupture and ground accelerations induced by CO<sub>2</sub> injection in the shallow crust. *Geophysical Journal International* **2012**, *190*, 1784–1789.
- Carroll, S. A.; Keating, E.; Mansoor, K.; Dai, Z.; Sun, Y.; Trainor-Guitton, W.; Brown, C.; Bacon, D. *Key Factors for Assessing Potential Groundwater Impacts Due to Leakage from Geologic Carbon Sequestration Reservoirs*; NRAP-TRS-I-003-2016; NRAP Technical Report Series; U.S. Department of Energy, National Energy Technology Laboratory: Morgantown, WV, 2016; p 40.
- Chang, K. W.; Minkoff, S. E.; Bryant, S. L. Simplified model for CO<sub>2</sub> leakage and its attenuation due to geological structures. *Energy Procedia* **2009**, *1*, 3453–3460.
- Chen, M.; Buscheck, T. A.; Wagoner, J. L.; Sun, Y.; White, J. A.; Chiaramonte, L.; Aines, R. D. Analysis of fault leakage from Leroy underground natural gas storage facility, Wyoming, USA. *Hydrogeology Journal* **2013**, *21*, 1429–1445.
- Convertito, V.; Maercklin, N.; Sharma, N.; Zollo, A. From induced seismicity to direct time-dependent seismic hazard. *Bulletin of the Seismological Society of America* **2012**, *102*, 2563–2573.
- Cornell, C. Engineering seismic risk analysis. *Bull. Seismol. Soc. Am.* **1968**, *59*, 1583–1606.
- Das, I.; Zoback, M. D. Long-period, long-duration seismic events during hydraulic stimulation of shale and tight-gas reservoirs—part 1: Waveform characteristics. *Geophysics* **2013**, *78*, KS97–KS108.
- Deichmann, N.; Giardini, D. Earthquakes Induced by the Stimulation of an Enhanced Geothermal System below Basel (Switzerland). *Seismol. Res. Letts.* **2009**, *80*, 784–798.
- Dieterich, J. Modeling of rock friction 1. Experimental results and constitutive equations. *Journal of Geophysical Research* **1979**, *84*, 2161–2168.
- Dieterich, J. U.C. Riverside. Personal communication, 2013.
- Dieterich, J.; Kilgore, B. Direct observation of frictional contacts: New insights for state-dependent properties. *Pure and Applied Geophysics* **1994**, *143*, 283–302.
- Dieterich, J.; Richards-Dinger, K. Earthquake recurrence in simulated fault systems. *Pure and Applied Geophysics* **2010**, *167*, 1087–1104.
- Douglas, J.; Edwards, B.; Sharma, N.; Tramelli, A.; Kraaijpoel, D.; Mena, B.; Maercklin, N.; Troise, C. Predicting ground motion from induced earthquakes in geothermal areas. *Bulletin of the Seismological Society of America* **2013**, *103*, 1875–1897.
- Dowding, C. *Construction Vibrations*; Prentice Hall, 1996.
- Eiken, O.; Ringrose, P.; Hermanrud, C.; Nazarian, B.; Torp, T.; Hoeir, L. Lessons learned from 14 years of CCS operations: Sleipner, In Salah, and Snøhvit. *Energy Procedia* **2011**, *4*, 5541–5548.
- Fault Analysis Group. 3D Relays from Seismic Data. University College Dublin, 2014. <http://www.fault-analysis-group.ucd.ie/gallery/3Drelay.htm>.
- FEMA. Federal Emergency Management Agency. Methodology for Estimating Potential Losses from Disasters, 2013. <http://www.fema.gov/hazus/#3>.

- Gan, W.; Frohlich, C. Gas injection may have triggered earthquakes in the Cogdell oil field, Texas. *Proceedings of the National Academy of Sciences* **2013**, *110*, 18786–18791.
- Gerstenberger, M.; Wiemer, S.; Giardini, D. A systematic test of the hypothesis that the b value varies with depth in California. *Geophysical Research Letters* **2001**, *28*, 57–60.
- Gerstenberger, M.; Wiemer, S.; Jones, L. *Real-time forecasts of tomorrow's earthquakes in California: A new mapping tool*; Open-file Report 2004-1390; U.S. Geological Survey, 2004.
- Gerstenberger, M.; Wiemer, S.; Jones, L.; Reasenber, P. Real-time forecasts of tomorrow's earthquakes in California. *Nature* **2005**, *435*, 328–331.
- Goertz-Allmann, B. P.; Wiemer, S. Geomechanical modeling of induced seismicity source parameters and implications for seismic hazard assessment. *Geophysics* **2012**, *78*, KS25–KS39.
- Graves, R. Simulating seismic wave propagation in 3D elastic media using staggered grid finite differences. *Bulletin of the Seismological Society of America* **1996**, *86*, 1091–1106.
- Graves, R.; Pitarka, A. Broadband ground-motion simulation using a hybrid approach. *Bulletin of the Seismological Society of America* **2010**, *100*, 2095–2123.
- Guglielmi, Y.; Cappa, F.; Amitrano, D. High-definition analysis of fluid-induced seismicity related to the mesoscale hydromechanical properties of a fault zone. *Geophysical Research Letters* **2008**, *35*, L06306.
- Gulia, L.; Wiemer, S. The influence of tectonic regimes on the earthquake size distribution: A case study for Italy. *Geophys. Res. Let.* **2010**, *37*.
- Gutenberg, B.; Richter, C. F. Earthquake magnitude intensity, energy, and acceleration. *Bull. Seismol. Soc. Am.* **1942**, *32*, 163–191.
- Hanks, T. C. Earthquake stress drops, ambient tectonic stresses and stresses that drive plate motions. *Pure and Applied Geophysics* **1977**, *115*, 441–458.
- Hartzell, S.; Guatteri, M.; Mai, P.; Liu, P.-C.; Fisk, M. Calculation of broadband time histories of ground motion, Part ii: Kinematic and dynamic modeling using theoretical Green's functions and comparison with the 1994 Northridge earthquake. *Bulletin of the Seismological Society of America* **2005**, *95*, 614–645.
- Hartzell, S.; Harmsen, S.; Frankel, A.; Larsen, S. Calculation of broadband time histories of ground motion: Comparison of methods and validation using strong ground motion from the 1994 Northridge earthquake. *Bulletin of the Seismological Society of America* **1999**, *89*, 1484–1504.
- Herak, M. ModelHSVR—a Matlab tool to model horizontal-to-vertical spectral ratio of ambient noise. *Computational Geosciences* **2008**, *34*, 1514–1526.
- Hutchings, L.; Ioannidou, E.; Kalogeras, I.; Voulgaris, N.; Savy, J.; Foxall, W.; Scognamiglio, L.; Stavrakakis, G. A physically based strong ground-motion prediction methodology; Application to PSHA and the 1999 M=6.0 Athens earthquake. *Geophysical Journal International* **2007**, *168*, 569–680.

- Hutchings, L.; Wu, F. Empirical Green's functions from small earthquakes: A waveform study of locally recorded aftershocks of the 1971 San Fernando Earthquake. *Journal of Geophysical Research* **1990**, *95*, 1187–1214.
- International Energy Agency. Energy Technology Perspectives 2010: Scenarios and Strategies to 2050; 2010.
- Jordan, P.; Oldenburg, C.; Nicot, J.-P. Estimating the probability of CO<sub>2</sub> plumes encountering faults. *Greenhouse Gases: Science and Technology* **2011**, *1*, 160–174.
- Kaplan, S.; Garrick, B. J. On the quantitative definition of risk. *Risk Analysis* **1981**, *1*, 11–27.
- Keranen, K.; Savage, H.; Abers, G.; Cochran, E. Potentially induced earthquakes in Oklahoma, USA: Links between wastewater injection and the 2011 MW 5.7 earthquake sequence. *Geology* **2013**. DOI:10.1130/G34045
- Kohli, A. H.; Zoback, M. D. Frictional properties of shale reservoir rocks. *Journal of Geophysical Research: Solid Earth* **2013**, *118*, 5109–5125.
- Kwiatak, G.; Plenkers, K.; Nakatani, M.; Yabe, Y.; Dresen, G.; JAGUARS-Group. Frequency-magnitude characteristics down to magnitude-4.4 for induced seismicity recorded at Mponeng Gold Mine, South Africa. *Bulletin of the Seismological Society of America* **2010**, *100*, 1165–1173.
- Majer, E.; Nelson, J.; Robertson-Tait, A.; Savy, J.; Wong, I. *Protocol for addressing induced seismicity associated with enhanced geothermal systems*; U.S. Department of Energy, DOE EE-0662; 2012a.
- Majer, E.; Nelson, J.; Robertson-Trait, A.; Savy, J.; Wong, I. *Best practices for addressing induced seismicity associated with enhanced geothermal systems (EGS)*; Draft report prepared for the DOE Geothermal Technologies Program, Lawrence Berkeley National Laboratory, 2012b.
- Marone, C.; Scholz, C. H. The depth of seismic faulting and the upper transition from stable to unstable slip regimes. *Geophysical Research Letters* **1988**, *15*, 621–624.
- Matzel, E. Seismic interferometry of the Salton Sea Geothermal Field. *Seismol. Res. Let.* **2012**, *83*, 465.
- Mazzoldi, A.; Rinaldi, A. P.; Borgia, A.; Rutqvist, J. Induced seismicity within geological carbon sequestration projects: Maximum earthquake magnitude and leakage potential from undetected faults. *International Journal of Greenhouse Gas Control* **2012**, *10*, 434–442.
- McCallen, D.; Astaneh-Asl, A.; Larsen, S.; Hutchings, L. Dynamic response of the suspension spans of the San Francisco-Oakland Bay Bridge. In Proceedings of the Eighth U.S. National Conference on Earthquake Engineering. EERI, 2006.
- McClure, M. W.; Horne, R. N. Investigation of injection-induced seismicity using a coupled fluid flow and rate/state friction model. *Geophysics* **2011**, *76*, WC181–WC198.
- McGarr, A. Maximum magnitude earthquakes induced by fluid injection. *Journal of Geophysical Research* **2014**, *119*, 1008–1019.

- Mena, B.; Wiemer, S.; Bachmann, C. Building robust models to forecast the induced seismicity related to geothermal reservoir enhancement. *Bulletin of the Seismological Society of America* **2013**, *103*, 383–393.
- Mori, J.; Abercrombie, R. E. Depth dependence of earthquake frequency-magnitude distributions in California: Implications for rupture initiation. *Journal of Geophysical Research* **1997**, *102*, 15081–15.
- National Research Council. *Induced Seismicity Potential in Energy Technologies*; National Academies Press, 2012.
- Ogata, Y. Seismicity analysis through point-process modeling: a review. *Pure Appl. Geophys.* **1999**, *155*, 471–507.
- Ogata, Y. Statistical-models for earthquake occurrences and residual analysis for point-processes. *Journal of the American Statistical Association* **1988**, *83*, 9–27.
- Pacala, S.; Socolow, R. Stabilization wedges: solving the climate problem for the next 50 years with current technologies. *Science* **2004**, *305*, 968–972.
- Pruess, K. Numerical studies of fluid leakage from a geologic disposal reservoir for co2 show self-limiting feedback between fluid flow and heat transfer. *Geophysical Research Letters* **2005**, *32*.
- Pulido, N.; Dalguer, L. Estimation of high-frequency radiation of the 2000 Tottori (Japan) earthquake based on dynamical model of fault rupture: Application to the strong ground motion simulation. *Bulletin of the Seismological Society of America* **2009**, *99*, 2305–2322.
- Reasenberg, P. A.; Jones, L. M. Earthquake hazard after a mainshock in California. *Science* **1989**, *243*, 1173–1176.
- Réveillère, A.; Rohmer, J.; Manceau, J-C. Hydraulic barrier design and applicability for managing the risk of CO<sub>2</sub> leakage from deep saline aquifers. *Int. J. Greenh. Gas Control* **2012**, *9*, 62–71.
- Richards-Dinger, K.; Dieterich, J. H. RSQSim earthquake simulator. *Seismological Research Letters* **2012**, *83*, 983–990.
- Rinaldi, A.; Rutqvist, J.; Cappa, F. Geomechanical effects on CO<sub>2</sub> leakage through fault zones during large-scale underground injection. *International Journal of Greenhouse Gas Control* **2014**, *20*, 117–131.
- Ruina, A. Slip instability and state variable friction laws. *Journal of Geophysical Research* **1983**, *88*, 359–10.
- Saikia, C. Modified frequency-wavenumber algorithm for regional seismograms using Filon's quadrature: Modeling of Lg waves in Eastern North America. *Geophysical Journal International* **1994**, *118*, 142–158.
- Scherbaum, F.; Hinzen, K.-G.; Ohrnberger, M. Determination of shallow shear wave velocity profiles in the Cologne, Germany area using ambient vibrations. *Geophysical Journal International* **2003**, *152*, 597–612.
- Scholz, C. H. *The Mechanics of Earthquakes and Faulting*; Cambridge University Press, 2002.

- Schorlemmer, D.; Wiemer, S.; Wyss, M. Variations in earthquake-size distribution across different stress regimes. *Nature* **2005**, *437*, 539–542.
- Schwartz, D. P.; Coppersmith, K. J. Fault behavior and characteristic earthquakes: Examples from the Wasatch and San Andreas fault zones. *Journal of Geophysical Research: Solid Earth (1978–2012)* **1984**, *89*, 5681–5698.
- Scognamiglio, L.; Hutchings, L. A test of a physically-based strong ground motion prediction methodology with the 27 September 1997, Mw = 6.0 Colfiorito (Umbria-Marcha sequence), Italy earthquake. *Tectonophysics* **2009**, *476*, 145–158.
- Segall, P. Earthquakes triggered by fluid extraction. *Geology* **1989**, *17*, 942–946.
- Shapiro, S. A.; Dinske, C. Fluid-induced seismicity: Pressure diffusion and hydraulic fracturing. *Geophysical Prospecting* **2009**, *57*, 301–310.
- Shapiro, S. A.; Dinske, C.; Kummerow, J. Probability of a given-magnitude earthquake induced by a fluid injection. *Geophys. Res. Lett.* **2007**, *34*.
- Shapiro, S.; Dinske, C.; Langenbruch, C.; Wenzel, F. Seismogenic index and magnitude probability of earthquakes induced during reservoir fluid stimulations. *Leading Edge* **2010**, *29*, 304–9.
- Shapiro, S.; Kruger, O.; Dinske, C.; Langenbruch, C. Magnitudes of induced earthquakes and geometric scales of fluid-stimulated rock volumes. *Geophysics* **2011**, *78*, WC55–WC63.
- Sibson, R. H. Fault zone models, heat flow, and the depth distribution of earthquakes in the continental crust of the United States. *Bulletin of the Seismological Society of America* **1982**, *72*, 151–163.
- Utsu, T. A statistical study on the occurrence of aftershocks. *Geophys Mag.* **1961**, *30*, 521–605.
- van Stiphout, T.; Kissling, E.; Wiemer, S.; Ruppert, N. Magmatic processes in the Alaska subduction zone by combined 3-D b value imaging and targeted seismic tomography. *J. Geophys. Res. - Solid Earth* **2009**, *114*, B11302.
- Wen, R.; Sinding-Larsen, R. Stochastic modelling and simulation of small faults by marked point processes and kriging. *Geostatistics Wollongong* **1997**, *96*, 398–414.
- Wibberley, C. A.; Yielding, G.; Di Toro, G. Recent advances in the understanding of fault zone internal structure: A review. *Geological Society, London, Special Publications* **2008**, *299*, 5–33.
- Wiemer, S.; Giardini, D.; Fäh, D.; Deichmann, N.; Sellami, S. Probabilistic seismic hazard assessment for Switzerland: best estimates and uncertainties. *J. of Seismology* **2009**, *13*, 449–478.
- Wiemer, S.; Wyss, M. Mapping the frequency-magnitude distribution in asperities: An improved technique to calculate recurrence times? *J. Geophys. Res. - Solid Earth* **1997**, *102*, 15115–15128.
- Working Group on California Earthquake Probabilities. *Earthquake probabilities in the San Francisco Bay Region: 2002–2031*; Open-file Report 03-214; U.S. Geological Survey, 2003.

- Youngs, R. R.; Coppersmith, K. J. Implications of fault slip rates and earthquake recurrence models to probabilistic seismic hazard estimates. *Bulletin of the Seismological society of America* **1985**, *75*, 939–964.
- Zhang, Y.; Oldenburg, C. M.; Finsterle, S. Percolation-theory and fuzzy rule-based probability estimation of fault leakage at geologic carbon sequestration sites. *Environmental Earth Sciences* **2010**, *59*, 1447–1459.
- Zoback, M. D.; Gorelick, S. M. Earthquake triggering and large-scale geologic storage of carbon dioxide. *Proceedings of the National Academy of Sciences* **2012**, *109*, 10164–10168.
- Zoback, M. L.; Zoback, M. State of stress in the conterminous united states. *Journal of Geophysical Research* **1980**, *85*, 6113–6156.
- Zoback, M.; Barton, C.; Brudy, M.; Castillo, D.; Finkbeiner, T.; Grollmund, B.; Moos, D.; Peska, P.; Ward, C.; Wiprut, D. Determination of stress orientation and magnitude in deep wells. *International Journal of Rock Mechanics and Mining Sciences* **2003**, *40*, 1049–1076.



NRAP is an initiative within DOE's Office of Fossil Energy and is led by the National Energy Technology Laboratory (NETL). It is a multi-national-lab effort that leverages broad technical capabilities across the DOE complex to develop an integrated science base that can be applied to risk assessment for long-term storage of carbon dioxide (CO<sub>2</sub>). NRAP involves five DOE national laboratories: NETL, Lawrence Berkeley National Laboratory (LBNL), Lawrence Livermore National Laboratory (LLNL), Los Alamos National Laboratory (LANL), and Pacific Northwest National Laboratory (PNNL).

### *Technical Leadership Team*

*Diana Bacon*

Lead, Groundwater Protection Working Group  
Pacific Northwest National Laboratory  
Richmond, WA

*Jens Birkholzer*

LBNL Lab Lead  
Lawrence Berkeley National Laboratory  
Berkeley, CA

*Grant Bromhal*

Technical Director, NRAP  
Research and Innovation Center  
National Energy Technology Laboratory  
Morgantown, WV

*Chris Brown*

PNNL Lab Lead  
Pacific Northwest National Laboratory  
Richmond, WA

*Susan Carroll*

LLNL Lab Lead  
Lawrence Livermore National Laboratory  
Livermore, CA

*Abdullah Cihan*

Lead, Reservoir Performance Working Group  
Lawrence Berkeley National Laboratory  
Berkeley, CA

*Tom Daley*

Lead, Strategic Monitoring Working Group  
Lawrence Berkeley National Laboratory  
Berkeley, CA

*Robert Dilmore*

NETL Lab Lead  
Research and Innovation Center  
National Energy Technology Laboratory  
Pittsburgh, PA

*Nik Huerta*

Lead, Migration Pathways Working Group  
Research and Innovation Center  
National Energy Technology Laboratory  
Albany, OR

*Rajesh Pawar*

LANL Lab Lead  
Lead, Systems/Risk Modeling Working Group  
Los Alamos National Laboratory  
Los Alamos, NM

*Tom Richard*

Deputy Technical Director, NRAP  
The Pennsylvania State University  
State College, PA

*Josh White*

Lead, Induced Seismicity Working Group  
Lawrence Livermore National Laboratory  
Livermore, CA



**Sean Plasynski**  
Executive Director  
Technology Development and  
Integration Center  
National Energy Technology Laboratory  
U.S. Department of Energy

**Heather Quedenfeld**  
Associate Director  
Coal Development and Integration  
National Energy Technology Laboratory  
U.S. Department of Energy

**Traci Rodosta**  
Technology Manager  
Strategic Planning  
Science and Technology Strategic Plans  
and Programs  
National Energy Technology Laboratory  
U.S. Department of Energy

**Mark Ackiewicz**  
Director  
Division of Carbon Capture and Storage  
Office of Fossil Energy  
U.S. Department of Energy

*NRAP Executive Committee*

**Cynthia Powell**  
Executive Director  
Research and Innovation Center  
National Energy Technology Laboratory

**Donald DePaolo**  
Associate Laboratory Director  
Energy and Environmental Sciences  
Lawrence Berkeley National Laboratory

**Roger Aines**  
Chief Energy Technologist  
Lawrence Livermore National  
Laboratory

**Melissa Fox**  
Program Manager  
Applied Energy Programs  
Los Alamos National Laboratory

**George Guthrie**  
Chair, NRAP Executive Committee  
Earth and Environmental Sciences  
Los Alamos National Laboratory

**Alain Bonneville**  
Laboratory Fellow  
Pacific Northwest National Laboratory

**Grant Bromhal**  
Technical Director, NRAP  
Senior Research Fellow  
Research and Innovation Center  
National Energy Technology Laboratory

